Identification of Linear Periodically Time-Varying (LPTV) Systems

A Thesis Submitted to the

College of Graduate Studies and Research

in Partial Fulfillment of the Requirements

for the degree of Master of Science

in the Department of Electrical and Computer Engineering

University of Saskatchewan

Saskatoon

By

Wutao Yin

Permission to Use

In presenting this thesis in partial fulfilment of the requirements for a Postgraduate degree from the University of Saskatchewan, I agree that the Libraries of this University may make it freely available for inspection. I further agree that permission for copying of this thesis in any manner, in whole or in part, for scholarly purposes may be granted by the professor or professors who supervised my thesis work or, in their absence, by the Head of the Department or the Dean of the College in which my thesis work was done. It is understood that any copying or publication or use of this thesis or parts thereof for financial gain shall not be allowed without my written permission. It is also understood that due recognition shall be given to me and to the University of Saskatchewan in any scholarly use which may be made of any material in my thesis.

Requests for permission to copy or to make other use of material in this thesis in whole or part should be addressed to:

Head of the Department of Electrical and Computer Engineering

57 Campus Drive

University of Saskatchewan

Saskatoon, Saskatchewan

Canada

S7N 5A9

ABSTRACT

A linear periodically time-varying (LPTV) system is a linear time-varying system with the co-efficients changing periodically, which is widely used in control, communications, signal processing, and even circuit modeling. This thesis concentrates on identification of LPTV systems. To this end, the representations of LPTV systems are thoroughly reviewed. Identification methods are developed accordingly. The usefulness of the proposed identification mehtods is verified by the simulation results.

A periodic input signal is applied to a finite impulse response (FIR)-LPTV system and measure the noise-contaminated output. Using such periodic inputs, we show that we can formulate the problem of identification of LPTV systems in the frequency domain. With the help of the discrete Fourier transform (DFT), the identification method reduces to finding the least-squares (LS) solution of a set of linear equations. A sufficient condition for the identifiability of LPTV systems is given, which can be used to find appropriate inputs for the purpose of identification.

In the frequency domain, we show that the input and the output can be related by using the discrete Fourier transform (DFT) and a least-squares method can be used to identify the alias components. A lower bound on the mean square error (MSE) of the estimated alias components is given for FIR-LPTV systems. The optimal training signal achieving this lower MSE bound is designed subsequently. The algorithm is extended to the identification of infinite impulse response (IIR)-LPTV systems as well. Simulation results show the accuracy of the estimation and the efficiency of the optimal training signal design.

Acknowledgements

I would like to thank my supervisor, Prof. Aryan Saadat Mehr, who guided me to this area of multirate signal processing. I have benefited tremendously from his great source of knowledge and his enthusiasm of doing research. I admire his knowledge of science, both in depth and broadness. I would like to thank Prof. Saadat Mehr for the large amount of time he has spent on the modification of my papers and thesis. He always proofreads my papers so carefully and gives me many insightful comments. Without his valuable advice, encouragement and unconditional support, this dissertation and the master work could not have been finished. Often times, I have realized how truly fortunate I am to have such an open-minded advisor who allowed me to choose my research subject freely. I am also grateful to Prof. Saadat Mehr's generous financial support.

I would like to thank my committee members: Prof. Richard Burton, Prof. Fang-Xiang Wu, and Prof. Sherif O. Faried for their valuable examinations and suggestions to improve the present work. I would like to express my great thanks to the professors who have given me various graduate courses. They are Prof. Yang Shi, Prof. Aryan Saadat Mehr, Prof. Fang-Xiang Wu, Prof. Daniel Teng, Prof. Anh v. Dinh, Prof. Li Chen, and Prof. Kunio Takaya. Especially, my sincere thanks go to Prof. Yang Shi and Prof. Fang-Xiang Wu both in academia and life philosophy.

I would like to express my gratitude to my parents Wengui Yin and Caimei Zhao for their selfless love and endless emotional support. I also credit my wife, Vicky J. Shi, for her thoughtful care and profound love. It is her unwavering love and unconditional support that inspire my life and work.

I also would like to thank the friends in Saskatoon. That is you people who make my stay here wonderful and cheerful. I also owe them a great deal for their friendship. I express gratitude to Huazhen Fang and Jiarui Ding for being inspiring friends, especially Huazhen who has been my classmate since college. I thank Yang Lin, Kuande Wang, Dongdong Chen, Yubo (Lele) She,

Hui Zhang, Yi Fang, Yu Zhang, Tao Wang, Bo Yu, Wenwen Yi, Alex X. Wang, Glen Wu, Lei Mu, Fei Gao, Xiuxin Yang, Yifang Wan, Chao Zhang for the beneficial discussions and wonderful hanging-out. Finally, my special thanks go to our host families–Laurel Kirkpatrick, Darin Kirkpatrick, Mervin Driedger, and Myrl Driedger, who made Saskatoon the second hometown for me.

Dedicate to my beloved parents.

Contents

List of Tables

LIST OF FIGURES

LIST OF ABBREVIATIONS

LPTV   Linear Periodically Time-Varying

LSTV   Linear Switched Time-Varying

LTI   Linear Time Invariant

MIMO   Multiple Input and Multiple Output

SISO   Single Input and Single Output

FIR   Finite Impulse Response

IIR   Infinite Impulse Response

ARMA   Autoregressive Moving Average

KLT   Karhunen-Loēve Transform

LMS   Least Mean Square

DFT   Discrete Fourier Transform

LS   Least Square

MSE   Mean Square Error

MMSE   Minimum Mean Square Error

CHAPTER 1

INTRODUCTION

1.1 Introduction to LPTV Systems

Linear periodically time-varying (LPTV) systems are widely used in control, communications, signal processing, and circuit modeling [1–43]. LPTV systems are a generalization of linear time-invariant (LTI) systems, that is, for an LPTV system with period M, when the input is delayed by M samples, so will be the output. From this point of view, an LTI system is an LPTV system with period 1. Moreover, a linear system that has coefficients changing periodically with period M is an LPTV system with period M. For an LTI system, the inputs and outputs of the system can be related by a transfer matrix. For a periodic system, we may use the blocked model of the system and obtain the alias-component matrix of the system, which relates the input and output of the system in the frequency domain [3].

There are many different ways to represent LPTV systems, each of which can be used to study certain aspects of these systems. Some common representations include Green function representation, multiple-input and multiple-output (MIMO) LTI models obtained by blocking, linear switched time-varying (LSTV) systems, and uniform maximally decimated multirate filter banks [1, 41, 44–55]. In Chapter 2, several representations will be discussed. These representations will be used later to study the identification of LPTV systems.

1.2 Previous Work on LPTV System Identification

Identification methods of LPTV systems have been proposed in [56–62] and the references therein. Next, we will review a number of the most representative works on identification of LPTV systems.

1

- **LPTV system identification in power systems:** An interpolating method is discussed in [56] which allows for efficient model identification in non-stationary power system conditions. The LPTV model of power systems is a reasonable extension of the LTI model and it has a clear physical explanation and mathematical description. The classical model description and identification is based on infinite impulse response (IIR) parametric model of tuned transfer function, with the LTI autoregressive moving average (ARMA) identification methods adapted to LPTV systems. The impulse excitation techniques and impulse response based LPTV system models deliver non-parametric model description, which can be easily changed to parametric ARMA formulation. Non-parametric description allows to use 2D interpolations in the frequency/relative time (f, t) domain with easy come-back as required by the LPTV model, time/relative time (t, t) domain. With the use of that approach the identification of the LPTV slowly varying structures is relatively quick, and the accuracy of identification is expected to be high.

- **Polyspectral analysis:** Polyspectral analysis is introduced to identify LPTV systems, e.g., [57], where nonparametric and parametric as well as non-stationary polyspectral estimation algorithms are discussed. These estimators are employed for identification of linear (almost) periodically time-varying systems for (almost) periodic signals and deterministic, stationary and non-stationary signals on a common high-order-statistics framework. All the methods are proven to be insensitive to stationary noise and employ consistent single record estimators.

- **Wavelets modeling and adaptive identification:** Wavelets modeling and adaptive identification methods have been investigated in [58, 63]. As for many stationary and non-stationary inputs the wavelet transform is claimed to be very close to the Karhunen-Loēve transform (KLT), which achieves exact diagonalization. A new approach for modeling discrete LPTV systems with finite impulse responses using wavelets is proposed. It shows that using wavelets can be viewed as a generalization of the raised model. A least mean square (LMS) based adaptive identification algorithm is discussed. This algorithm is simple, and has reasonable

tracking abilities and low computational complexity. The motivation behind this algorithm is to separate parameters, similar to frequency domain LMS. Its main disadvantage, as is well known, is its slow convergence. This disadvantage becomes more acute here, since compared to LTI systems, time-scale for any adaptive algorithm is lower for LPTV systems, by a factor equal to their period.

- **Finite basis decomposition:** Modeling of linear systems by basis functions can turn a time-varying system identification into a time-invariant one. For that purpose, the power series, Legendre polynomial basis, wavelet basis, and prolate spheroidal basis can be used to model LPTV systems. Another motivation for using basis functions is that some linear systems can be represented with fewer coefficients than when using standard modeling (e.g., for time-invariant systems, by modeling the corresponding spectrum by rational functions). In this case, system identification can be easier and more efficient. Several works can be found in [59] and its references therein.

- **State-space model:** Several state-space model based identification methods are proposed in the references [60, 61, 64–66]. Several subspace[60, 64–66] based identification methods are developed to identify linear parameter varying systems. In [61], the authors discussed the identification of LPTV systems in the framework of sample data systems. With the state-space model representation, many control methods can be applied to identify LPTV systems. Controllability and observability of LPTV systems are studied from the perspective of control theory accordingly.

1.3   Outline of the Thesis

In Chapter 1, a brief introduction to LPTV systems is given. We also review the previous work on LPTV system identification.

In Chapter 2, we review several representations of LPTV systems. Difference equations, Green function, LSTV, alias components, MIMO-LTI, and maximally decimated filter banks representa-

tion have been fully discussed as each representation can reveal certain aspect of an LPTV system. These different representations form the basis of the following chapters, and also act as a tutorial.

In Chapter 3, we derive a new method for the identification of discrete LPTV systems. An LPTV system with period M is considered. If an input with period N is applied to this system, where N is a multiple of M, the output of the system will be periodic with period N. Using periodic inputs, we show that we can formulate the problem of identification of LPTV systems in the frequency domain. With the help of the discrete Fourier transform (DFT), the identification method reduces to finding the least-squares (LS) solution of a set of linear equations. A sufficient condition for the identifiability of LPTV systems is given, which can be used to find appropriate inputs for the purpose of identification. Simulation results illustrate the efficiency of the proposed algorithm.

In Chapter 4, an LS method for identifying alias components of discrete LPTV systems is proposed. We apply a periodic input signal to an LPTV system and measure the noise-contaminated output. We show that the input and output can be related by using the DFT. In the frequency domain, a least-squares method can be used to identify the alias components. A lower bound on the mean square error (MSE) of estimated alias components is given for FIR-LPTV systems. The optimal training signal achieving this lower MSE bound is designed subsequently. The algorithm is extended to the identification of infinite impulse response (IIR)-LPTV systems as well. Simulation results show the accuracy of the estimation and the efficiency of the optimal training design.

In Chapter 5, we summarize and draw some concluding remarks from the thesis research. Suggestions for some future work are presented as well in this chapter.

Notation: The notation used throughout the thesis is fairly standard. $(\cdot)^T$, $(\cdot)^*$, $(\cdot)^H$, and $(\cdot)^\dagger$ denote transpose, conjugate, conjugate transpose, and Moore-Penrose pseudo-inverse, respectively. The symbol W_N is equal to $e^{-\jmath 2\pi/N}$, where $\jmath = \sqrt{-1}$ and similarly for W_M. In the whole thesis, N generally stands for the period of the input signal and M for the period of the LPTV system. The DFT coefficients of $x(n)$ are denoted by $X[k]$, and the $N \times N$ DFT matrix is denoted by $[\boldsymbol{F}_N]_{mn} = W_N^{mn}, m, n \in \{0, 1, \cdots, N-1\}$. A Gaussian random variable with mean μ and variance

σ^2 is denoted by $z \sim \mathcal{N}(\mu, \sigma^2)$. The Euclidean norm of a vector $\boldsymbol{x}$ is denoted as $\|\boldsymbol{x}\|$. $\lfloor X \rfloor$ stands for the largest integer less than or equal to X. The $N \times N$ identity matrix is represented by $\boldsymbol{I}_N$. The operator $\otimes$ is used to represent the Kronecker product. Bold-faced quantities denote matrices and vectors.

CHAPTER 2

LPTV SYSTEMS REVIEW

There are many different ways to represent LPTV systems, each of which can be used to study certain aspects of these systems. Some common representations include Green function, MIMO LTI models obtained by blocking, LSTV systems, and uniform maximally decimated multirate filter banks [1, 41, 44–53]. In the following, we will study these representations as we will be using them for the identification of LPTV systems later on.

2.1   Green function

Green function representation is used as a general expression for a linear time-varying system. (The system is not necessarily periodically time-varying.) Here, we consider a periodic-M LPTV system $\mathcal{G}$. The input x and the output y of the LPTV system can be related by

$$
\begin{aligned}
y(n) &= \sum_{l=-\infty}^{\infty} g(n,l)x(l) \\
&= \sum_{l=-\infty}^{\infty} h(n, n-l)x(l) \\
&= \sum_{l=-\infty}^{\infty} f(l, n-l)x(l),
\end{aligned}
\tag{2.1}
$$

where $g(n,l)$ is the response of the system at time n to an impulse applied at time l in its input, i.e., the Green function. Here, another form Green function can be defined by variables substitution

$$
h(n,l) \triangleq g(n, n-l),
$$

and

$$
f(n,l) \triangleq g(n+l, l).
$$

6

Here, $h(n,l)$ and $f(n,l)$ represent, respectively , the system response at time n due to an unit impulse applied at time $n-l$, and the response at time $n+l$ due to an unit impulse applied at time l. Figure 2.1 gives a structure figure to show the relationships among $g(n,l)$, $h(n,l)$, and $f(n,l)$. Here, $h(k,p)$ is the pth element of the kth *column* of $h(n,l)$, and $f(k,p)$ is the pth element of the kth *row* of $h(n,l)$, with columns and rows zero-referenced from the main diagonal of $h(n,l)$ as shown in Figure 2.1.
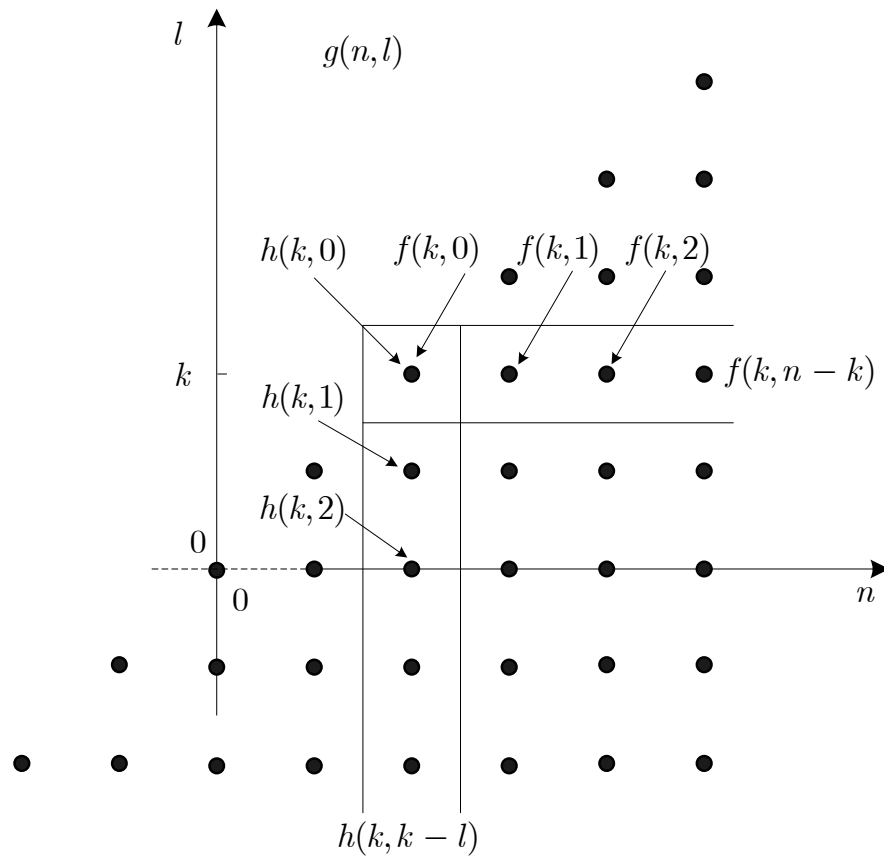
Figure 2.1: Green function structure of an LPTV system.

Now for an LPTV system with period M, due to the periodic condition on the system, it is not

difficult to show that the impulse response has the property

$$g(n + M, l + M) = g(n, l), \quad \forall k, l$$

$$h(n + M, l) = h(n, l), \quad \forall k, l \tag{2.2}$$

$$f(n + M, l) = f(n, l), \quad \forall k, l$$

This results clearly show that there are only M unique rows and M unique columns in $h(n, l)$, and arithmetic mod-M operator $\langle \rangle$ should be approximately used in all the previous expressions, thus giving

$$
\begin{aligned}
y(n) &= \sum_{l=-\infty}^{\infty} g(n, l)x(l) \\
&= \sum_{l=-\infty}^{\infty} h\left(\langle n \rangle, n - l\right) x(l) \\
&= \sum_{l=-\infty}^{\infty} f(\langle l \rangle, n - l)x(l),
\end{aligned}
\tag{2.3}
$$

with

$$h(k, l) = f(\langle k - l \rangle, l) = h(k, k - l)$$

$$f(k, n) = h(\langle k + n \rangle, n) = h(k + n, k), \quad 0 \le k \le M - 1.$$

2.2 Difference Equation

LPTV discrete-time system with period M is a system for which a shift in the input sequence by M samples results in a shift of M samples in the output sequence. These systems are a generalization of LTI systems. Therefore, like LTI systems, LPTV systems can also be formulated by a difference equation. For an LPTV system $\mathcal{G}$, we can use a difference equation to represent it as follows

$$y(n) = \sum_{i=0}^{M-1} a_i(n)x(n - i) - \sum_{i=1}^{M-1} b_i(n)y(n - i), \tag{2.4}$$

where

$$a_i(n) = a_i(n - M), \quad i = 0, 1, \cdots, M - 1$$

$$b_i(n) = b_i(n - M), \quad i = 1, 2, \cdots, M - 1.$$

Figure 2.2 gives a time-varying IIR filter-like structure for the difference equation representation in (2.4). Equation (2.4) uses a set of time-invariant coefficients to give
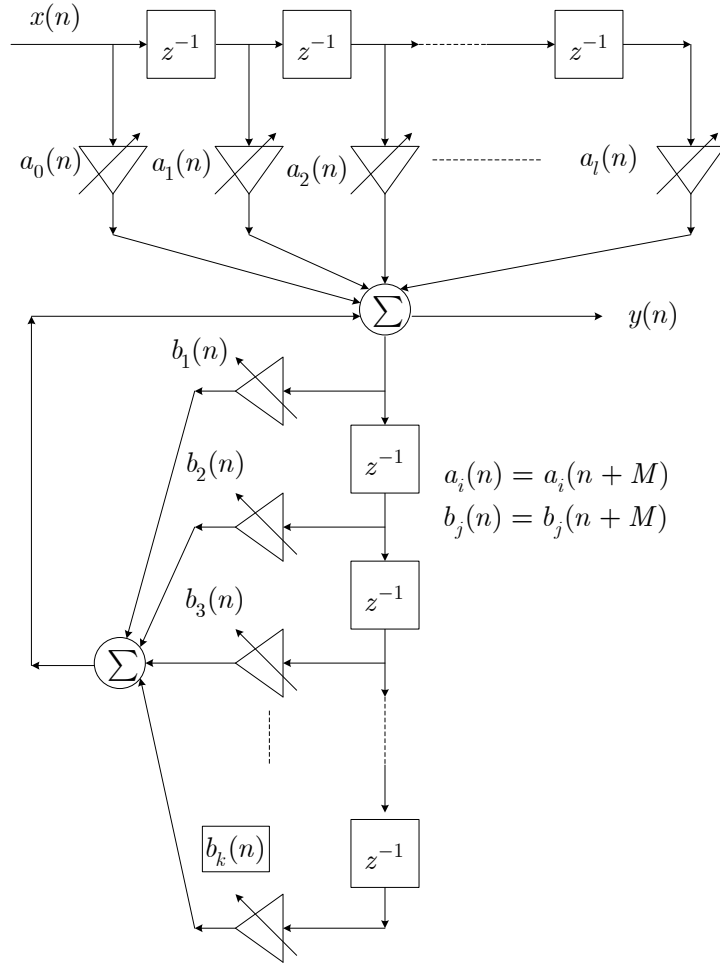
Figure 2.2: Difference equation representation of an LPTV system.

$$y_k(n) = \sum_{i=0}^{M-1} a_{ik}(n)x_{\langle k-i\rangle}(n + \langle k - i\rangle) + \sum_{j=1}^{M-1} b_{jk}(n)y_{\langle k-i\rangle}(n + \langle k - i\rangle),$$

$$k = 0, 1, \cdots, M - 1, \quad (2.5)$$

where

$$\begin{cases} x_k(n) = x(nM + k), & -\infty \le n \le \infty \\[2mm] y_k(n) = y(nM + k), & 0 \le k \le M - 1 \\[2mm] a_{ik} = a_i(k) = a_i(nM + k), & 0 \le i \le M - 1 \\[2mm] b_{jk} = b_j(k) = b_j(nM + k), & 0 \le i \le M - 1 \end{cases}$$

with the brackets $\langle \cdot \rangle$ relating to the arithmetic modulo-M. The LPTV difference equation in (2.4)

9

has now been transformed into M equivalent LTI systems, but crosscoupled. We also see that equation (2.5) corresponds the structure in Figure 2.5. Once taking the z-transform of each one of these linear difference equations in (2.5) results in M linear simultaneous equations in the M z-transforms of the subsampled outputs of $y(n)$, i.e., $Y_k(z), k = 0, 1, \cdots, M-1$. These simultaneous equations can now be solved to give [49]

$$\boldsymbol{Y}(z) = \bar{\mathcal{F}}(z)\boldsymbol{X}(z),$$

where $\boldsymbol{Y}(z)$ and $\boldsymbol{X}(z)$ is a column vector formed by their M-phase decomposition terms, and $\bar{\mathcal{F}}(z)$ is given in equation (2.11).

2.3 Linear Switched Time-Varying

By defining $h(m, i) = g(m, m - i)$, we can write (2.1) as

$$y(m) = \sum_{i=0}^{\infty} h(m, m - i)x(i),$$

Using (2.2), we have

$$h(m, i) = h(m + M, i).$$

Setting

$$H_m(z) = \sum_{i=0}^{\infty} h(m, i)z^{-i}$$

and noting that $H_m = H_{m+M}$, we obtain a representation of an LPTV system by M LTI subsystems and a commutative switch at the output as shown in Figure 2.3a (which is an LSTV setting [45]). The switch is connected to the output of the first LTI subsystem H_0 at time 0, to the output of H_1 at time 1, and to H_{M-1} at time $M - 1$, and then, it repeats and connects to H_0. Meanwhile, the similar structure given in Figure 2.3b can also be obtained by setting

$$f(l, k) = g(l + k, l).$$

The M-periodic condition on the LPTV system $\mathcal{G}$ gives

$$f(l, k) = f(l + M, k).$$
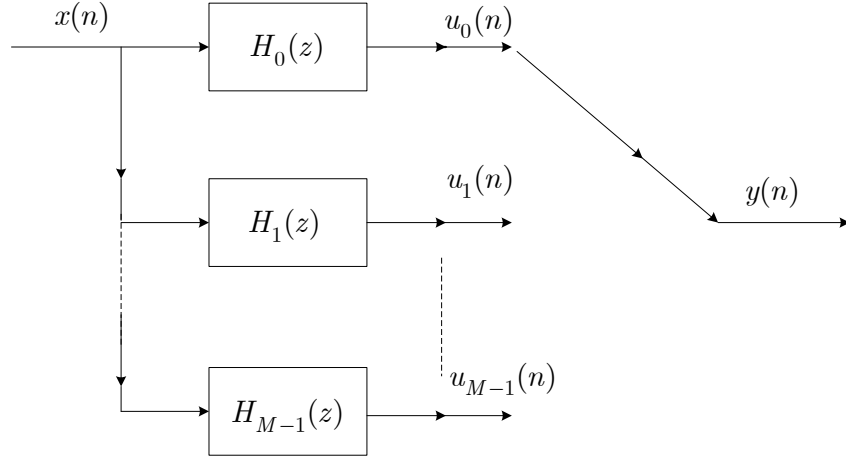
(a) Output switch
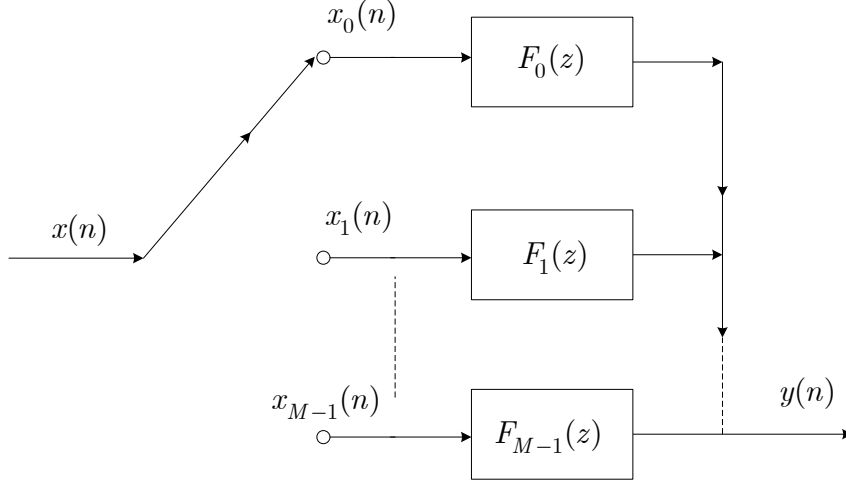
(b) Input switch

Figure 2.3: Structure of an LSTV system with (2.3a) output switch and (2.3b) input switch.

By substituting f for g in (2.1), we get

$$
\begin{aligned}
y(k) &= \sum_{i=-\infty}^{k} f(i, k-i)u(i) \\
&= \sum_{l=0}^{p-1} \sum_{r=-\infty}^{\infty} f(l, k-l-rp)u(l+rp).
\end{aligned}
\tag{2.6}
$$

Define the LTI systems

$$
F_l(z) = \sum_{k=0}^{\infty} f(l, k)z^{-k}.
$$

Because of the M-periodic condition, $F_l = F_{l+M}$, and we see that (2.6) is equivalent to the LSTV system shown in Figure 2.3b.

2.4 Alias Components

Consider the LSTV system $\{H_0, H_1, \cdots, H_{M-1}\}_o$ in Figure 2.3a, where $_o$ stands for the output switch. The switch can be substituted by directly connecting the input to branches and introducing a multiplication factor in each branch that is zero at all sampling times that the switch is not connected to the branch and is equal to 1 when it is connected, i.e., for branch i , we multiply the input by

$$\frac{1}{M} \sum_{l=0}^{M-1} W_M^{(n-i)l}, \tag{2.7}$$

where $W_M = e^{-2\pi j/M}$. Note that the results in (2.7) is nonzero only when n is an integer multiple of i, that is

$$\frac{1}{M} \sum_{l=0}^{M-1} W_M^{(n-i)l} = \begin{cases} 1, & \text{if } n \text{ is a multiple of } i \\ \\ 0, & \text{otherwise} \end{cases}$$

As the multiplication by W_M^{-kn} in the time domain is equivalent to a shift in frequency by $2\pi k/M$ in the frequency domain, the output of the LPTV system $Y(z)$ and its input $X(z)$ are related by

$$\begin{aligned} Y(z) &= \frac{1}{M} \sum_{i=0}^{M-1} \sum_{l=0}^{M-1} W_M^{-il} F_i(z) X(z W_M^{-l}) \\ &= \sum_{l=0}^{M-1} \left(\sum_{i=0}^{M-1} \frac{1}{M} W_M^{-il} F_i(z) \right) X(z W_M^{-l}). \end{aligned} \tag{2.8}$$

By writing

$$A_l = \sum_{i=0}^{M-1} \frac{1}{M} W_M^{-il} F_i(z),$$

the system $\mathcal{G}$ can be represented as shown in Figure 2.4.

If we define

$$\boldsymbol{X}^T(z) = \left[X(z), X(z W_M^{-1}), \cdots, X\left(z W_M^{-M+1}\right) \right], \tag{2.9}$$

and

$$\boldsymbol{A}^T(z) = [A_0(z), A_1(z), \cdots, A_{M-1}(z)],$$

equation (2.8) can be written as

$$Y(z) = \boldsymbol{X}^T(z) \boldsymbol{A}(z). \tag{2.10}$$
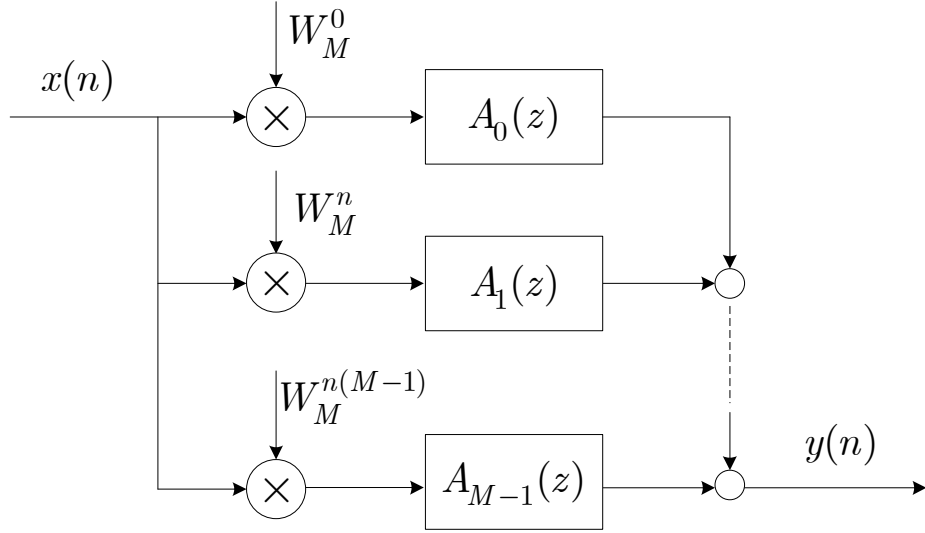
Figure 2.4: Alias components representation for an LPTV system $\mathcal{G}$.

The subsystem A_i yields the transfer function from the frequency shifted input $X(zW_M^i)$ to the output $Y(z)$. This is in contrast with an LTI system that has an input-output relationship given by $Y(z) = A_0(z)X(z)$. The difference system $A - A_0$ represents the alias components, and its norm gives a measure of the alias distortions in an LPTV system [67].

2.5   MIMO LTI Model

Defining the blocking (or lifting) of an input sequence $x(n)$ into a sequence of vectors of length M as [29, 45, 68]

$$x(n) = [x(nM), x(nM + 1), \cdots, x(nM + M - 1)]^T,$$

we consider an LPTV system $\mathcal{G}$ with the LSTV representation $\{F_0, F_1, \cdots, F_{M-1}\}_i$, where $_i$ denotes an input switch shown in Figure 2.3b. If the input and output sequences are blocked into sequences of vectors of length M , an equivalent LTI system $\underline{\mathcal{F}}$ results as shown in Figure 2.5. Note that in Figure 2.5 $x_l(z)$ and $y_l(z), 0 \leq l \leq M-1$ denote the lth polyphase of $x(n)$ and $y(n)$, respectively. The system $\underline{\mathcal{F}}$ has M inputs and M outputs. The (i, l)th element of the polyphase matrix $\underline{\mathcal{F}}(z)$ gives the transfer function between the lth component of the blocked input and the ith component
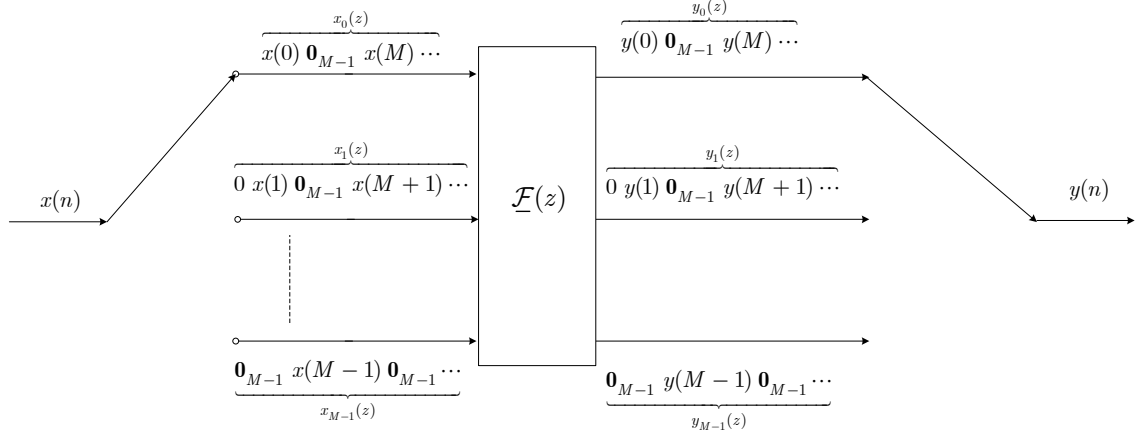
Figure 2.5: Equivalent MIMO-LIT system for an LPTV system $\mathcal{F}$ with an input switch.

of the blocked output. Because of the switch, the lth component of the blocked input is only connected to the subsystem F_l. By writing $F_l(z)$ in terms of its polyphase components as

$$F_l(z) = \sum_{i=0}^{p-1} z^{-i} F_i^l(z^p),$$

we have

$$\underline{\mathcal{F}}_{(i,l)}(z) = \begin{cases} F_{i-l}^l(z), & \text{if } l \le i \\ z^{-1} F_{M-l+i}^l(z) & \text{otherwise.} \end{cases}$$

Therefore, the transfer matrix of the equivalent MIMO-LIT system can be written as follows

$$\underline{\mathcal{F}}(z) = \begin{bmatrix} F_0^0(z) & z^{-1} F_{M-1}^1(z) & \cdots & z^{-1} F_1^{M-1}(z) \\ F_1^0(z) & F_1^1(z) & \cdots & z^{-1} F_2^{M-1}(z) \\ \vdots & \vdots & \ddots & \vdots \\ F_{M-1}^0(z) & F_{M-2}^1(z) & \cdots & F_0^{M-1}(z) \end{bmatrix}. \tag{2.11}$$

This can be intuitively explained as we take the lth column of the polyphase matrix of the lth branch $F_l(z)$ shown in Figure 2.3b and form an equivalent polyphase matrix for the LPTV system $\mathcal{G}$.

Similarly, when an output switch structure $\{H_0, H_1, \cdots, H_{M-1}\}_i$ shown in Figure 2.3a is considered, the blocked representation of this system can be found by noting that the element (i, l) of the polyphase matrix $\underline{\mathcal{H}}$ is the output of the LTI system H_i at time $kp + l$ for an integer k. Take

14

H_l^i to be the polyphase components of H_i as in

$$H_l(z) = \sum_{i=0}^{p-1} z^{-i} H_i^l(z^p).$$

Figure 2.6 shows the structure diagram. The polyphase components of H_i appear on the ith row of the polyphase matrix, and we have

$$\underline{\mathcal{H}}(z) = \begin{bmatrix} H_0^0(z) & z^{-1}H_{M-1}^0(z) & \cdots & z^{-1}H_1^0(z) \\ H_1^1(z) & H_0^1(z) & \cdots & z^{-1}H_2^1(z) \\ \vdots & \vdots & \ddots & \vdots \\ H_{M-1}^{M-1}(z) & H_{M-2}^{M-1}(z) & \cdots & H_0^{M-1}(z) \end{bmatrix}. \tag{2.12}$$

2.6 State-Space Model

As mentioned in [14, 69], an LPTV system can also be represented by a state-space model as follows

$$x(n+1) = A(n)x(n) + b(n)u(n) \tag{2.13}$$

$$y(n) = c(n)x(n) + d(n)u(n), \tag{2.14}$$

where $x(n)$ is an M-dimensional state vector, $u(n)$ is the scalar input, $y(n)$ is the scalar output, and $A(n), b(n), c(n)$, and $d(n)$ are respectively $M \times M$, $M \times 1$, $1 \times M$ and 1×1 real matrices with
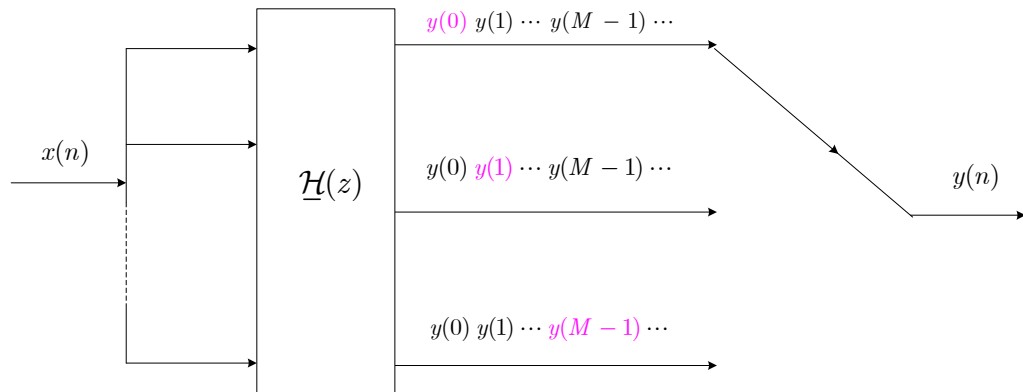
Figure 2.6: Equivalent MIMO-LIT system for an LPTV system $\mathcal{G}$ with an output switch.
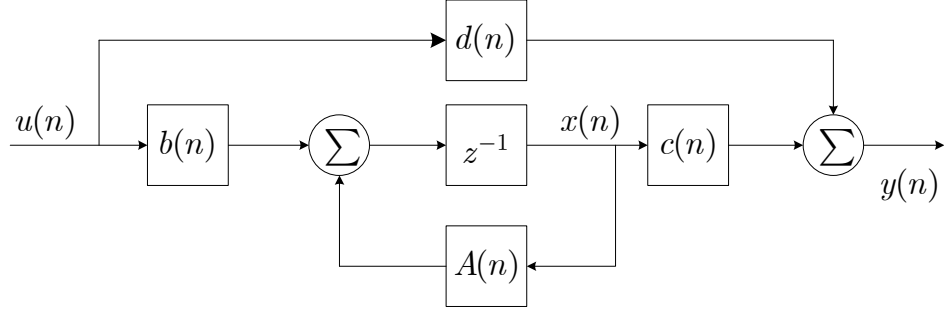
Figure 2.7: LPTV state-space digital filter.

period M as follows

$$A(n + M) = A(n), b(n + M) = b(n)$$

$$c(n + M) = c(n), d(n + M) = d(n).$$

The signal flow graph of this LPTV state-space digital filter is shown in Figure 2.7. The unit impulse response $h(n, k)$ of this LPTV state-space digital filter, which is the output at time n when the input is the unit impulse at time k, can be evaluated as follows:

$$h(n, k) = \begin{cases} 0 & n < k \\ d(k) & n = k \\ c(n)b(k) & n = k + 1 \\ c(n) \displaystyle\prod_{i=k+1}^{n-1} A(i)b(k) & n > k + 1. \end{cases}$$

Note that the impulse response varies periodically with period M for n and k as $h(n, k) = h(n + M, k + M)$.

2.7 Maximally Decimated Filterbanks

By using the multirate building blocks, we can get a filter banks representation of an LPTV system. Consider the representation given in Figure 2.3b. Due to the switch, the output of an LPTV system at time $rM + m$, $y(rM + m)$ is equal to the output of the mth branch $u_m(rM + m)$, where $0 \le m \le M - 1$ and r is an integer.
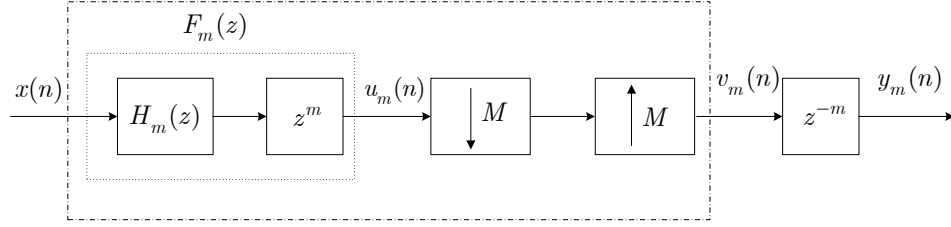
Figure 2.8: The mth branch of an LPTV system.
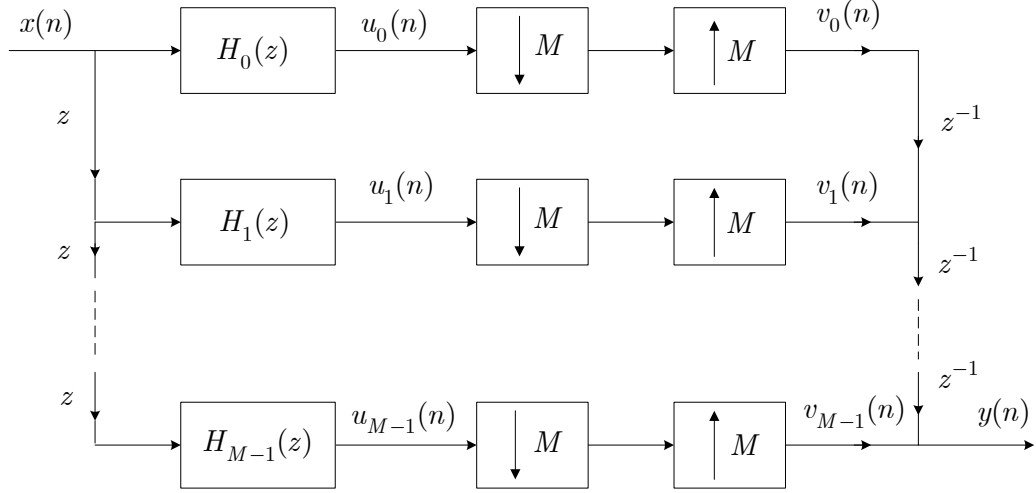
Figure 2.9: Equivalent filter banks for an LPTV system.

We can represent the mth branch by a filter and some multirate building blocks, i.e., a time delay block z^{-m}, a downsampler by M, $\downarrow M$, an upsampler by M, $\uparrow M$, and a time advance block z^m, given in Figure 2.8: A downsampler by M is used to decrease the sampling rate of an input signal by keeping every Mth sample, while an upsampler by M is used to increase the sampling rate of an input signal by inserting $M - 1$ zeros between samples. The combination of z^m, downsampler by M, upsampler by M and z^{-m} fulfills the task of keeping the $rM + m$th samples of $u_m(n)$ unchanged and setting others 0. Because the block $H_m(z)$ and z^{-m} can commute, we can rearrange an LPTV system as a multirate filter bank shown in Figure 2.9, which is an equivalent setting to the LSTV structure given in Figure 2.3b.

17

2.8 Conclusion

In this chapter we discussed the various representations of LPTV systems, i.e., Green functions, difference equation, linear switched time varying, alias components, MIMO LTI, state-space, and maximally decimated filterbanks. These different representations are the basis of the identification algorithms in the following chapters. It is noted that throughout this thesis we will discuss the identification of an LPTV system based on the several aforementioned LPTV representations.

CHAPTER 3

IDENTIFICATION OF LPTV SYSTEMS BY USING AN LSTV REPRESENTATION

In the previous chapter, we reviewed various representations of LPTV systems. These representations revealed different aspects of an LPTV system. In this chapter, we focus on the LSTV representation and develop an identification method based on this structure.

3.1   Introduction

Identification methods of LPTV systems have been proposed in [56–61] and the references therein: An interpolating method is discussed in [56] which allows for efficient model identification in non-stationary power system conditions. Polyspectral analysis is introduced to identify LPTV systems, e.g., [57], where nonparametric and parametric as well as non-stationary polyspectral estimation algorithms are discussed. Wavelets modeling and identification methods have been investigated in [58, 59], while subspace based method is developed in [60]. The authors in [61] discussed the identification of LPTV systems in the framework of sample data system.

In this chapter, we develop an identification method for discrete single-input single-output (SISO) LPTV systems by using periodic inputs. The approach goes as follow: Take a finite impulse response LPTV system with period M. A periodic input with period N is applied, where N is an integer multiple of M. After the system has reached the steady state, the output signal will also have a period of N. White Gaussian noise is added to the output of this LPTV system. As there is no frequency leakage, the DFT can be applied to the input and the output. We show that when N is greater than the number of the parameters to be estimated, an overdetermined system is formed

and our identification method reduces to finding the LS solution of a set of linear equations [70]. Then, a sufficient condition for identifiability is derived based on a multirate filter bank structure. Finally, when compared with the least-mean-square (LMS) algorithm, the proposed algorithm gives more accurate results. It is straightforward to generalize this method to MIMO LPTV systems. Therefore, we will focus on the SISO LPTV in the following.

The rest of this chapter is organized as follows. Section 3.2 describes the basic LPTV system model. Section 3.3 presents the identification method and discusses the identifiability conditions. Numerical simulation results of the proposed method are given in section 3.4, and the conclusion is in Section 3.5.

3.2   System Model

Take an LPTV system with period M. It is a causal system. The input x and the output y of the LPTV system are related by

$$y(m) = \sum_{i=0}^{\infty} g(m,i)x(i), \tag{3.1}$$

where $g(m,i)$ is the response of the system at time m to an impulse applied at time i in its input, i.e., the Green function. Due to the inherent periodic property of LPTV systems, we have

$$g(m+M, i+M) = g(m,i), \quad \forall m, i. \tag{3.2}$$

By defining $h(m,i) = g(m, m-i)$, we can write (3.1) as

$$y(m) = \sum_{i=0}^{\infty} h(m, m-i)x(i),$$

Using (3.2), we have

$$h(m,i) = h(m+M, i).$$

Setting

$$H_m(z) = \sum_{i=0}^{\infty} h(m,i)z^{-i}$$

and noting that $H_m = H_{m+M}$, we obtain a representation of an LPTV system by M LTI subsystems and a commutative switch at the output as shown in Figure 3.1 (which is an LSTV setting [45]).

The switch is connected to the output of the first LTI subsystem H_0 at time 0, to the output of H_1 at time 1, and to H_{M-1} at time $M - 1$, and then, it repeats and connects to H_0. Therefore, an LPTV system can be fully characterized by M LTI subsystems. If $H_0 = H_1 =, \cdots, = H_{M-1}$, an LPTV system will reduce to an LTI system. Here, we assume the impulse response of each subsystem is of finite length.
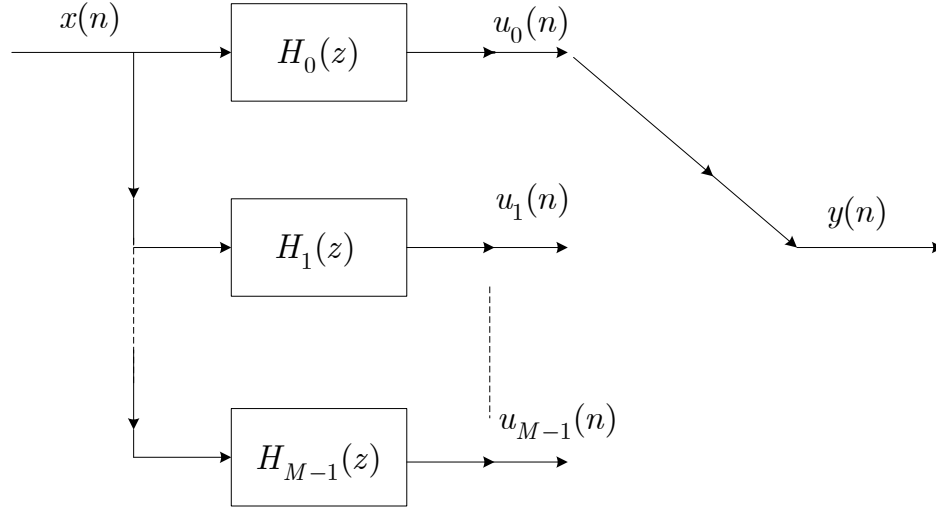
Figure 3.1: An LPTV system with period M and a commutative switch at the output.

Given the LPTV system above, the commutative switch can be substituted by connecting the output of the LTI subsystems to the branches and introducing a multiplication factor in each branch that is zero when the switch is not connected to the branch and is equal to 1 when it is connected, i.e., for branch m, the output of the mth LTI subsystem at time n is multiplied by the factor

$$\frac{1}{M} \sum_{\ell=0}^{M-1} W_M^{(n-m)\ell}.$$

Thus, in the frequency domain the output $Y(z)$ is obtained as [44, 45, 71]

$$Y(z) = \sum_{m=0}^{M-1} Y_m(z), \tag{3.3}$$

where

$$Y_m(z) = \frac{1}{M} \sum_{\ell=0}^{M-1} W_M^{-m\ell} H_m(zW_M^{-\ell}) X(zW_M^{-\ell}). \tag{3.4}$$

21

As $H_m(z)$ is assumed to be of finite length, we can denote it as

$$H_m(z) = \sum_{i=0}^{L_m-1} h(m,i)z^{-i} = \boldsymbol{e}_m^T(z)\boldsymbol{h}_m, \tag{3.5}$$

where

$$\boldsymbol{e}_m^T(z) \triangleq [1, z^{-1}, \cdots, z^{-(L_m-1)}],$$

$$\boldsymbol{h}_m^T \triangleq [h(m,0), h(m,1), \cdots, h(m, L_m - 1)],$$

and L_m is the length of the m-th branch.

Substituting (3.5) into (3.4) gives

$$\begin{aligned} Y_m(z) &= \frac{1}{M} \sum_{\ell=0}^{M-1} W_M^{-m\ell} X(zW_M^{-\ell}) \boldsymbol{e}_m^T(zW_M^{-\ell})\boldsymbol{h}_m \\ &= \left[c_m^{(0)}(z), c_m^{(1)}(z), \cdots, c_m^{(L_m-1)}(z) \right] \boldsymbol{h}_m \end{aligned}, \tag{3.6}$$

where we define

$$c_m^{(i)}(z) \triangleq \frac{1}{M} \sum_{\ell=0}^{M-1} W_M^{-m\ell}(zW_M^{-\ell})^{-i} X(zW_M^{-\ell}). \tag{3.7}$$

Thus, defining

$$\boldsymbol{c}_m^T(z) \triangleq \left[c_m^{(0)}(z), c_m^{(1)}(z), \cdots, c_m^{(L_m-1)}(z) \right], \tag{3.8}$$

we have

$$Y_m(z) = \boldsymbol{c}_m^T(z)\boldsymbol{h}_m. \tag{3.9}$$

Putting everything together, we get

$$Y(z) = \boldsymbol{c}^T(z)\boldsymbol{h}, \tag{3.10}$$

where

$$\boldsymbol{h}^T \triangleq [\boldsymbol{h}_0^T, \boldsymbol{h}_1^T, \cdots, \boldsymbol{h}_{M-1}^T],$$

$$\boldsymbol{c}^T(z) \triangleq [\boldsymbol{c}_0^T(z), \boldsymbol{c}_1^T(z), \cdots, \boldsymbol{c}_{M-1}^T(z)].$$

Next, we will discuss how to estimate the impulse response of an LPTV system by using (3.10).

22

3.3 Algorithm Description and Analysis

In this section, we will describe the proposed algorithm. Identifiability conditions will be discussed as well, i.e. a sufficient condition for the input signal design is presented. Based on this condition, we can design an input sequence to make sure an FIR LPTV system is identifiable.

3.3.1 Algorithm Description

Consider an LPTV system with period M (see Figure 3.1) and assume that the impulse response of every branch is of finite length as given in the previous section. We apply a random input of period N to this LPTV system, where N is an integer multiple of M, i.e., $N = KM$. After the system has reached the steady state, the output of the LPTV system is also of period N because each subsystem is an LTI system. Note that the system reaches the steady-state in L_{max} sampling time, where L_{max} is the maximum length of impulse response of all the subsystems, i.e.,

$$L_{max} = \max_{m}\{L_m\}.$$

Here, the steady state means that after several periods of input, the output will also be periodic. It's different from the definition of the linear system theory. As both the input and the output signals are periodic, we can take the DFT of the input and the output signals without any frequency leakage. Therefore, the estimation will be more precise than an aperiodic input. Before going further, we denote N consecutive input samples in one period as

$$\boldsymbol{x} = [x(0), x(1), \cdots, x(N-1)]^T,$$

and N consecutive output samples in one period as

$$\boldsymbol{y} = [y(0), y(1), \cdots, y(N-1)]^T.$$

Here, evaluating (3.10) at frequency $\omega_k = 2\pi k/N$ (i.e., by substituting $z = W_N^{-k}$) gives [72]

$$Y(W_N^{-k}) = \boldsymbol{c}^T(W_N^{-k})\boldsymbol{h}, \tag{3.11}$$

where

$$Y(W_N^{-k}), k = 0, 1, \cdots, N - 1,$$

are the DFT coefficients of the output, denoted by $Y[k]$.

Defining $c_m^{(i)}[k] \triangleq c_m^{(i)}(W_N^{-k})$, we have

$$
\begin{aligned}
c_m^{(i)}[k] &= \frac{1}{M} \sum_{\ell=0}^{M-1} W_M^{-m\ell} (W_N^{-k} W_M^{-\ell})^{-i} X(W_N^{-k} W_M^{-\ell}) \\
&= \frac{1}{M} \sum_{\ell=0}^{M-1} W_N^{-\ell K(m-i)+ki} X \left(W_N^{-(k+\ell K)} \right) \\
&= \frac{1}{M} \sum_{\ell=0}^{M-1} W_N^{-\ell K(m-i)+ki} X[k + \ell K]
\end{aligned}
\tag{3.12}
$$

where

$$X[k + \ell K] \triangleq X \left(W_N^{-(k+\ell K)} \right).$$

Note that $X[k]$ and $Y[k]$ are periodic with period N, and they are the N-point DFT coefficients of $x(n)$ and $y(n)$, respectively. Next we will show that after some evaluations, equation (3.11) can be used to identify LPTV systems.

Using (3.8) and (3.12) gives

$$\boldsymbol{c}_m^T[k] \triangleq \boldsymbol{c}_m^T(W_N^{-k}) = \left[c_m^{(0)}[k], c_m^{(1)}[k], \cdots, c_m^{(L_m-1)}[k] \right].$$

Therefore, (3.11) can be rewritten as

$$Y[k] = \boldsymbol{c}^T[k]\boldsymbol{h}, \tag{3.13}$$

where

$$\boldsymbol{c}^T[k] \triangleq \left[\boldsymbol{c}_0^T[k], \boldsymbol{c}_1^T[k], \cdots, \boldsymbol{c}_{M-1}^T[k] \right].$$

Generally, there is some noise present while measuring the output signal. The noise is usually assumed to be an identical independently distributed (i.i.d.) Gaussian random variable with zero mean and variance σ^2. Considering the measuring and system noise, we write (3.13) in a matrix form as follows

$$\mathcal{Y} = \mathcal{C}\boldsymbol{h} + \boldsymbol{w}, \tag{3.14}$$

where

$$
\mathcal{Y} = \begin{bmatrix} Y[0] \\ Y[1] \\ \vdots \\ Y[N-1] \end{bmatrix}, \quad \boldsymbol{h} = \begin{bmatrix} \boldsymbol{h}_0 \\ \boldsymbol{h}_1 \\ \vdots \\ \boldsymbol{h}_{M-1} \end{bmatrix},
$$

and

$$
\mathcal{C} = \begin{bmatrix} \boldsymbol{c}_0^T[0] & \boldsymbol{c}_1^T[0] & \cdots & \boldsymbol{c}_{M-1}^T[0] \\ \boldsymbol{c}_0^T[1] & \boldsymbol{c}_1^T[1] & \cdots & \boldsymbol{c}_{M-1}^T[1] \\ \vdots & \vdots & \ddots & \vdots \\ \boldsymbol{c}_0^T[N-1] & \boldsymbol{c}_1^T[N-1] & \cdots & \boldsymbol{c}_{M-1}^T[N-1] \end{bmatrix}.
$$

Here, the vector $\boldsymbol{w}$ is the N-point DFT of the noise which accounts for the measuring error and system noise, and the matrix $\mathcal{C}$ has a dimension of $N \times L$, where

$$
L \triangleq \sum_{m=0}^{M-1} L_m.
$$

As the input is known, the elements of the data matrix $\mathcal{C}$ can be found. Note that there are L unknown parameters and a set of N linear equations in (3.14). If $N < L$, equation (3.14) is underdetermined and the parameters can not be identified uniquely. For $N \geq L$, unless the matrix $\mathcal{C}$ is rank deficient, the parameters can be identified without error when the noise $\boldsymbol{w} = \boldsymbol{0}$. In this case, the matrix $\mathcal{C}$ has full column rank, and we can find $\boldsymbol{h}$ by

$$
\boldsymbol{h} = \mathcal{C}^\dagger \mathcal{Y}, \tag{3.15}
$$

where

$$
\mathcal{C}^\dagger = (\mathcal{C}^H \mathcal{C})^{-1} \mathcal{C}^H.
$$

If the noise $\boldsymbol{w} \neq 0$, then

$$
\boldsymbol{h} = \mathcal{C}^\dagger \mathcal{Y} - \mathcal{C}^\dagger \boldsymbol{w}. \tag{3.16}
$$

For a fixed signal to noise ration (SNR), we can improve the estimation error by increasing N.

Now, let $\hat{\boldsymbol{h}}$ denote the optimal estimation of $\boldsymbol{h}$. In the 2-norm sense, finding the optimal solution to (3.14) is equivalent to minimizing the residue $\mathcal{Y} - \mathcal{C}\boldsymbol{h}$ over $\boldsymbol{h}$, that is,

$$
\hat{\boldsymbol{h}} = \arg \min_{\boldsymbol{h}} \|\mathcal{Y} - \mathcal{C}\boldsymbol{h}\|^2. \tag{3.17}
$$

Accordingly, given $\mathcal{Y}$ and $\mathcal{C}$, the parameters that minimize (3.17) are given by the LS estimator

$$\hat{\boldsymbol{h}} = \mathcal{C}^{\dagger}\mathcal{Y}. \tag{3.18}$$

3.3.2 Identifiability Conditions

In this section, we will first discuss a filter bank representation of LPTV systems. Then, we will use this representation to study the identifiability of LPTV systems.

Take the representation given in Figure 3.1. Due to the switch, the output of an LPTV system at time $rM + m$, $y(rM + m)$ is equal to the output of the mth branch $u_m(rM + m)$, where $0 \leq m \leq M - 1$ and r is an integer. We can represent the mth branch by a filter and some multirate building blocks, i.e., a time delay block z^{-m}, a downsampler by M, $\downarrow M$, an upsampler by M, $\uparrow M$, and a time advance block z^m, given in Figure 3.2: A downsampler by M is used to decrease the sampling rate of an input signal by keeping every Mth sample, while an upsampler by M is used to increase the sampling rate of an input signal by inserting $M - 1$ zeros between samples. The combination of z^m, downsampler by M, upsampler by M and z^{-m} fulfills the task of keeping the $rM + m$th samples of $u_m(n)$ unchanged and setting others 0. Because the block $H_m(z)$ and z^{-m} can commute, we can rearrange an LPTV system as a multirate filter bank shown in Figure 3.3, which is an equivalent setting to the LSTV structure given in Figure 3.1. Next, we will use this structure to discuss the identifiability of LPTV systems.
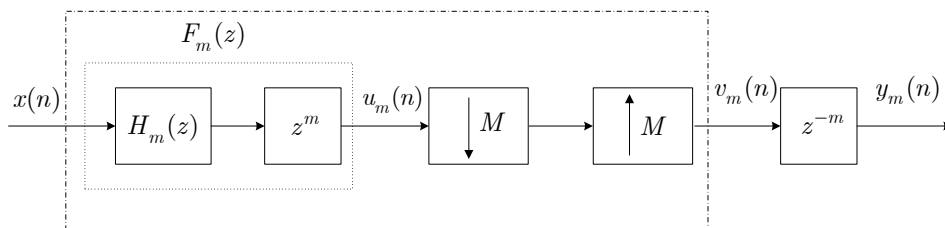
Figure 3.2: The mth branch of a periodic-M LPTV system.

First of all, we will simplify this problem by making use of the special structure of LPTV systems. Consider the structure shown in Figure 3.3: the output samples $y(n)$ in every M consecutive samples are from M different branches, which means those M branches can be treated separately. At the

same time, all the branches share the same structure and have the same input. Therefore, it is reasonable for us to investigate the identifiability for one branch. If all branches of an LPTV system are identifiable, the whole system will be identifiable.
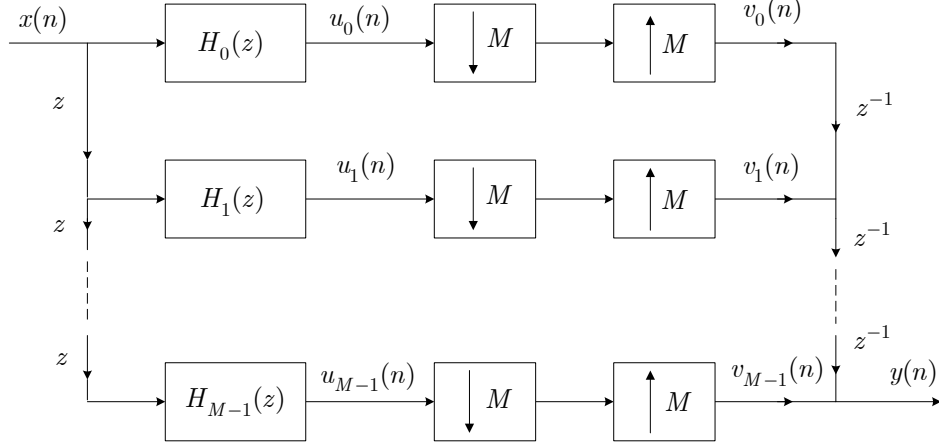
Figure 3.3: A filter bank representation of a periodic-M LPTV systems.

In the following, we will focus on one branch to investigate the identifiability. Without loss of generality, we pick the mth branch of an LPTV system (see Figure 3.2). Because the time delay block z^{-m} and the advance block z^m don't affect the identifiability, we can concentrate on the blocks in the dash-dotted box, and furthermore absorb the block z^m into the LTI system $H_m(z)$, denoted by $F_m(z) = z^m H_m(z)$ (i.e., the two blocks in the dotted box). Now, we relate $x(n)$ to $v_m(n)$ in the frequency domain as follows

$$V_m(z) = \frac{1}{M} \sum_{\ell=0}^{M-1} F_m(zW_M^\ell) X(zW_M^\ell). \tag{3.19}$$

Following the method we used in section 3.3.1, evaluating (3.19) at the frequency $\omega_k = 2\pi k/N$ (i.e., by substituting $z = W_N^{-k}$) gives

$$\begin{aligned}
V_m[k] &= \frac{1}{M} \sum_{\ell=0}^{M-1} F_m(W_N^{-k+\ell K}) X(W_N^{-k+\ell K}) \\
&= \frac{1}{M} \sum_{\ell=0}^{M-1} F_m(W_N^{-k+\ell K}) X[k - \ell K]
\end{aligned}, \tag{3.20}$$

where $V_m[k]$ is the N-point DFT coefficients of $v_m(n)$ and is periodic with period-N.

In order to make an LPTV system identifiable, we will impose a constraint on the DFT coefficients of the input signal $x(n)$ as follows. This condition will not ensure $x(n)$ is a real signal instead

of a complex one, but we will comment on this later on.

$$
\underline{Condition}: \quad
\begin{cases}
X[k] \neq 0, & 0 \leq k \leq K-1 \\
\\
X[k] = 0, & \text{otherwise}
\end{cases}, \tag{3.21}
$$

where those consecutive nonzero K inputs will lead to alias-free outputs. Given the condition (3.21) and equation (3.20), we can obtain at most K distinct linear equations as follows

$$
V_m[k] = \frac{1}{M} F_m(W_N^{-k}) X[k], \quad 0 \leq k \leq K-1. \tag{3.22}
$$

Reformulating (3.22) in a matrix form gives

$$
\mathcal{V}_m = \Pi^m \boldsymbol{X}_D \boldsymbol{F}_{K \times L} \boldsymbol{h}_m, \tag{3.23}
$$

where

$$
\mathcal{V}_m \triangleq [V_m[0], V_m[1], \cdots, V_m[K-1]]^T
$$

$$
\Pi \triangleq \mathrm{diag}\{1, W_N^{-1}, \cdots, W_N^{-(K-1)}\} \qquad .
$$

$$
\boldsymbol{X}_D \triangleq \mathrm{diag}\{X[0], X[1], \cdots, X[K-1]\}
$$

In the above, the symbol Π^m is the mth power of the matrix Π, $\mathrm{diag}\{\boldsymbol{A}\}$ represents diagonal matrix formed from the vector $\boldsymbol{A}$, and $\boldsymbol{F}_{K \times L_m}$ is a $K \times L_m$ submatrix of an $N \times N$ DFT matrix $\boldsymbol{F}_{N \times N}$ at the top left corner .

From equation (3.22), it is seen that the identifiability of the mth branch is equivalent to judging whether the matrix $\Pi^m \boldsymbol{X}_D \boldsymbol{F}_{K \times L_m}$ has a full column rank. Note that the diagonal matrices Π^m and $\boldsymbol{X}_D$ are obviously invertible, and the matrix $\boldsymbol{F}_{K \times L_m}$ is a Vandermonde matrix with its rank given by $\min\{K, L_m\}$. Therefore, we can obtain that the $K \times L_m$ matrix $\Pi^m \boldsymbol{X}_D \boldsymbol{F}_{K \times L_m}$ has a rank of $\min\{K, L_m\}$. We can come to a conclusion that if $K \geq L_m$, the parameter $\boldsymbol{h}_m$ can be uniquely identified, namely, the mth branch is identifiable for $\forall m \in \{0, 1, \cdots, M-1\}$. Given the aforementioned discussion, the whole system is identifiable if every branch is identifiable, i.e., $K \geq L_{max}$, where $L_{max} = \max_m L_m$. Under the condition (3.21), once this LPTV system is identifiable, we can also have $K \geq L_{max}$. Therefore, $K \geq L_{max}$ is a necessary condition under the condition (3.21).

As mentioned before, under the condition (3.21) the input signal $x(n)$ will not be real. If the input sinal must be real, we just need to make the DFT coefficients sequence $X[k], 0 \leq k \leq N-1$

a Hermitian sequence

$$X[k] = X^*[N-k], \quad 0 \leq k \leq N-1$$

where this could be considered as a frequency shift of condition (3.21). Therefore, (3.21) can be

rewritten as

$$X[k] \neq 0, \quad -\lfloor K/2 \rfloor \leq k \leq \lfloor K/2 \rfloor \tag{3.24}$$

where $X[k] = X^*[N-k]$. Note that we consider $X[0]$ and $X[N-1]$ as adjacent elements. Because

the frequency shift only relates to an exponential factor, the identifiability will not be affected

accordingly. Therefore, a real signal will always exist. As an underlying condition, K must be an

odd number to make the input signal $X[k]$ a Hermitian sequence. If K is an even number, the

input signal $x(n)$ is not a real signal under the condition (3.21).

The condition we give in equation (3.21) is a sufficient one. In general, it will not be a necessary

condition. However, based on this sufficient condition, we can design the input sequence to make

sure an LPTV system is identifiable. Moreover, the input sequence given in (3.21) can cancel

the alias components of an LPTV system, which will reduce the computational complexity of

the identification algorithm. From the point view of identifiability, a sufficient condition is more

important than a necessary one. When we do the numerical simulation, we find that in almost every

trial randomly generated sequences can make an LPTV system identifiable, which can be intuitively

interpreted as a random sequence that is rich enough in modes [73]. However, the simulation results

also demonstrate our sufficient condition is conservative.

3.4 Numerical Examples

In this section, we will give an explicit example to demonstrate our method and compare our

simulation results with those obtained by the LMS algorithm (see sections 5.2 in [74] for more

details). In order to apply the LMS algorithms, we need to block this periodic-M LPTV system

to an $M \times M$ MIMO LTI system, i.e., the raised model [58, 71]. As is known, an $M \times M$ MIMO

system can be considered to be blocked by M multi-input single-output (MISO) system. To make

this section self-contained, we include the MIMO-LTI model here once again.
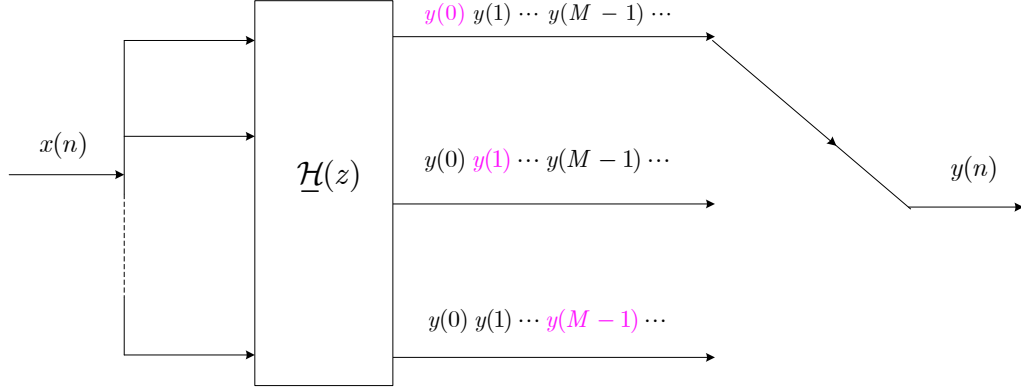
Figure 3.4: Equivalent MIMO-LIT system for an LPTV system $\mathcal{G}$ with an output switch.

When an LPTV system $\{H_0, H_1, \cdots, H_{M-1}\}_i$ shown in Figure 2.3a, the blocked representation of this system can be found by noting that the element (i, l) of the polyphase matrix $\underline{\mathcal{H}}$ is the output of the LTI system H_i at time $kp + l$ for an integer k. Take H_l^i to be the polyphase components of H_i as in

$$H_l(z) = \sum_{i=0}^{p-1} z^{-i} H_i^l(z^p).$$

The polyphase components of H_i appear on the ith row of the polyphase matrix, and we have

$$\underline{\mathcal{H}}(z) = \begin{bmatrix} H_0^0(z) & z^{-1} H_{M-1}^0(z) & \cdots & z^{-1} H_1^0(z) \\ H_1^1(z) & H_0^1(z) & \cdots & z^{-1} H_2^1(z) \\ \vdots & \vdots & \ddots & \vdots \\ H_{M-1}^{M-1}(z) & H_{M-2}^{M-1}(z) & \cdots & H_0^{M-1}(z) \end{bmatrix}. \tag{3.25}$$

In this stage, the LMS algorithm can be applied to those M MISO systems directly [58]. We will first define SNR and the normalized mean square error (NMSE) as follows

$$\mathsf{SNR} = \frac{\|\boldsymbol{y}\|^2}{N\sigma^2}$$

and

$$\mathsf{NMSE} = \frac{\|\hat{\boldsymbol{h}} - \boldsymbol{h}\|^2}{\|\boldsymbol{h}\|^2}$$

We take an LPTV system with period $M = 2$. The corresponding frequency response of each

branch is as follows

$$\begin{cases} H_0(z) = 0.3 + 0.1z^{-1} + 0.05z^{-2} + 1.25z^{-3} \\ \\ H_1(z) = 0.4 - 0.05z^{-1} - 0.01z^{-2} + 0.8z^{-3} \end{cases}$$

Hence, the parameters to be estimated can be written as a vector

$$\boldsymbol{h} = [0.3 \ 0.1 \ 0.05 \ 1.25 \ 0.4 \ -0.05 \ -0.01 \ 0.8]^T.$$

3.4.1 Performance of the Proposed Algorithm

We consider an input signal $\boldsymbol{x}$ with period N and take the input and the output samples in 1 period. We assume that $\boldsymbol{x}$ is known. However, in order to test different cases, we have generated a periodic input randomly. Gaussian noise with zero mean at $\mathsf{SNR} = 25\mathsf{dB}$ is added to the output of the above LPTV system. Taking $N = 100$, we obtain that the corresponding ensemble average NMSE is 2.2737×10^{-4} using the proposed method. The estimation results are given in Table 3.1(a).

Table 3.1: Identification results for the two algorithms

Subsystem	Estimated Coefficients			
H_0	[0.3087	0.0990	0.0605	1.2516]
H_1	[0.4108	-0.0541	0.0004	0.7886]

(a) The proposed algorithm

Subsystem	Estimated Coefficients			
H_0	[0.3016	0.0763	0.0614	1.2401]
H_1	[0.4074	-0.0564	-0.0141	0.7969]

(b) The LMS algorithm

3.4.2 Performance of the LMS Algorithm

Table 3.1(b) demonstrates the simulation results by employing the LMS algorithm at $\mathsf{SNR} = 25\mathsf{dB}$. Here, the step size is taken as $\mu = 0.05$ (see the explicit expressions in [74]). In this example, the LMS algorithm converges after 250 input samples. The corresponding ensemble average NMSE is

3.7055×10^{-4} when the LMS algorithm converges. The frequency responses of $H_0(z)$ and $H_1(z)$ are given in Figure 3.5. In Figure 3.5, solid line is for true value, dashed for the proposed algorithm, dotted for the LMS algorithm with the step size $\mu = 0.05$ and dashdot for the LMS algorithm with $\mu = 0.01$.

(a) Frequency response for $H_0(z)$

(b) Frequency response for $H_1(z)$
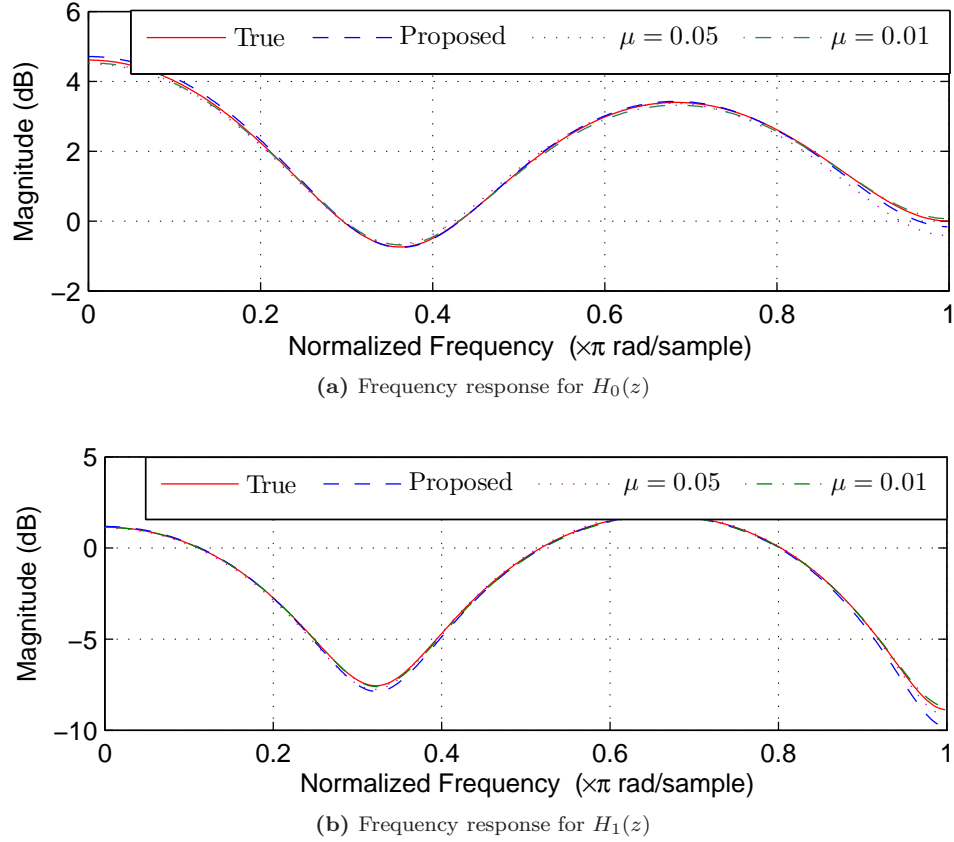
Figure 3.5: Frequency responses for $H_0(z)$ and $H_1(z)$.

Here, the input periodical signal is also generated randomly as the input for the LMS algorithm. The ensemble average learning curve is illustrated in Figure 3.6. For the LMS algorithm, the horizontal axis stands for the number of input samples for the iteration, while for the proposed method the horizontal axis denotes the period of the input signal (only one period of the output is used for the identification). Examining the figure, we can see that the proposed method is better than the LMS algorithms in this example. In order to investigate the method, we have repeated the process for LPTV systems with different periods and FIR filter coefficients many times. We observed that the MSE curves of our method stay below those of the LMS algorithms, which means

that our method needs shorter training sequences and has a lower mean squares error.
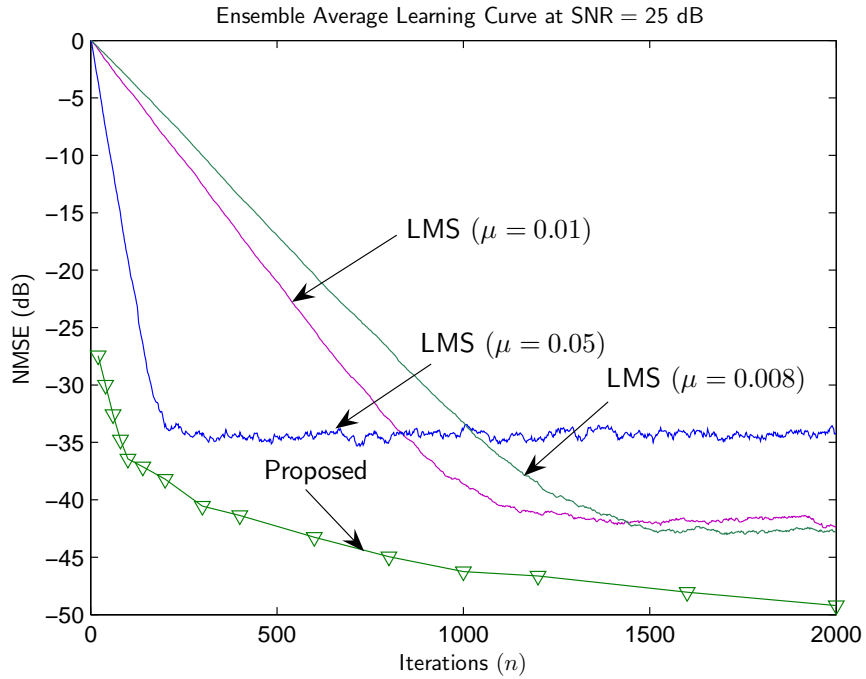
Figure 3.6: NMSE curve for the two algorithms.

3.5   Conclusion

We derived a method for the identification of FIR LPTV systems in the frequency domain by using DFT. We chose the period of the input signal to be a multiple of the period of an LPTV system. Then, the output of the system has the same period as the period of the input signal. Therefore, our identification method reduces to finding the least-squares solution of a set of linear equations. A sufficient condition for the identifiability is given, which can be used to find appropriate inputs for the purpose of identification. Simulation results illustrated the accuracy of the proposed method. A comparison with the LMS algorithms was presented as well.

Chapter 4

Alias Components Identification of LPTV Systems

In Chapter 3, we discussed the identification method based on an LSTV structure. In this chapter, we will develop an identification method for LPTV system by using the alias components representation in the frequency domain.

4.1 Introduction

In general, there are two ways to represent LPTV systems in a wide sense: one is a time-domain based approach called blocking in signal processing, and the other one is a frequency-domain technique [45, 49, 71]. These two techniques are inherently related. In this chapter, for the convenience of discussion we adopt the latter one, which is modelled as alias components in parallel with frequency shifted inputs shown in Figure 4.1. A key question for system identification is how to choose the training signal [75]. Especially, optimal training signal design is very important in communication area [76–80], to name a few. However, they generally deal with LTI systems. To the best of the authors' knowledge, the optimal training signal design for the identification of LPTV systems has not been studied.

In this chapter, we develop an identification method for alias components of discrete FIR-LPTV systems. Take an FIR-LPTV system with period M. A periodic training signal with period N is applied, where N is a multiple of M, so in the steady-state, the output will also have period N. We measure the output of this LPTV system. Due to the periodicity of the input and the output, the DFT can be applied to the input and the output signals. Therefore, when N is greater than the

number of the parameters to be estimated, an overdetermined system is formed. This identification method is equivalent to solving a LS problem [70, 75]. Because the alias component representation is a frequency-domain representation, we feel that is more natural to derive the equations in the frequency domain. However, the algorithm can be derived in the time domain, in which case, an LSTV setup [45] can be used. But we should note that in the time domain representation the input signal does not have to be periodic. Therefore, the two methods are not exactly equivalent. In order to evaluate the proposed method, an MSE lower bound on this LS estimator is derived. An optimal training signal is designed to achieved this lower bound as well. Finally, this algorithm is extended to the identification of IIR-LPTV systems.

The rest of this chapter is organized as follows. Section 4.2 introduces the alias component representation of LPTV systems. Section 4.3 presents the least-squares identification of alias components for FIR-LPTV systems. Section 4.4 describes the optimal input signal design for FIR-LPTV systems in the sense of minimum MSE (MMSE). An extension to IIR-LPTV system identification is presented in Section 4.5. Numerical simulation results of the proposed method are given in Section 4.6, and the conclusion is in Section 4.7.

4.2 System Model

Take an LPTV system $\mathcal{A}$ with period M. Such a system can be modelled as M alias components with periodic modulating inputs. Figure 4.1 shows the alias components representation of an LPTV system, where $A_m(z), m = 0, \cdots, M-1$ are its alias components [44]. Given the LPTV system in Figure 4.1, in the frequency domain the output $Y(z)$ is obtained as [44, 45]

$$Y(z) = \sum_{m=0}^{M-1} A_m(z) X(zW_M^{-m}), \tag{4.1}$$

where the quantities $A_m(z)$ are the alias components of the aforementioned LPTV system and $X(zW_M^{-m})$ can be considered as the input of $A_m(z)$. If we define

$$\boldsymbol{X}^T(z) = \left[X(z), X(zW_M^{-1}), \cdots, X\left(zW_M^{-M+1}\right) \right], \tag{4.2}$$

35
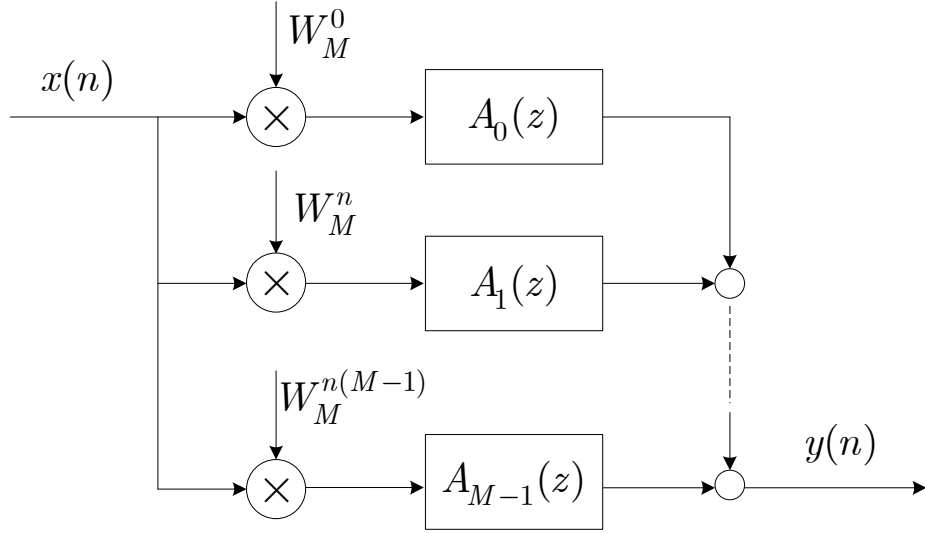
Figure 4.1: Alias component representation of an LPTV system.

and

$$\boldsymbol{A}^T(z) = [A_0(z), A_1(z), \cdots, A_{M-1}(z)],$$

equation (4.1) can be written as

$$Y(z) = \boldsymbol{X}^T(z)\boldsymbol{A}(z). \tag{4.3}$$

Assume that the impulse responses of the LPTV system, i.e., the response to impulses at time 0 to $M - 1$, are shorter than L. Because the alias components $A_m(z), m = 0, 1, \cdots, M - 1$ are a linear transformation of the impulse responses, i.e., alias components are the DFT of the impulse responses [45], the length of alias components will also be less than L. Hence, we can denote $A_m(z)$ as

$$A_m(z) = \sum_{i=0}^{L-1} a_{m,i} z^{-i} = \boldsymbol{\alpha}_m^T \boldsymbol{e}(z), \tag{4.4}$$

where

$$\boldsymbol{\alpha}_m^T \triangleq [a_{m,0}, a_{m,1}, \cdots, a_{m,L-1}],$$

and

$$\boldsymbol{e}^T(z) \triangleq [1, z^{-1}, \cdots, z^{-(L-1)}].$$

If $A_m(z), m = 0, \cdots, M - 1$ are of different lengths, zeros can be padded to make sure they have

the same length. Without loss of generality, we consider they have the same length L.

Substituting (4.4) into (4.3) gives

$$
\begin{aligned}
Y(z) &= \boldsymbol{X}^T(z) \left[\boldsymbol{\alpha}_0^T \boldsymbol{e}(z), \boldsymbol{\alpha}_1^T \boldsymbol{e}(z), \cdots, \boldsymbol{\alpha}_{M-1}^T \boldsymbol{e}(z) \right]^T \\
&= \boldsymbol{X}^T(z) \left(\boldsymbol{I}_M \otimes \boldsymbol{e}^T(z) \right) \boldsymbol{\alpha} \\
&= \boldsymbol{\varphi}^T(z)\boldsymbol{\alpha},
\end{aligned}
\tag{4.5}
$$

where

$$
\boldsymbol{\alpha}^T \triangleq \left[\boldsymbol{\alpha}_0^T, \boldsymbol{\alpha}_1^T, \cdots, \boldsymbol{\alpha}_{M-1}^T \right],
$$

$$
\boldsymbol{\varphi}^T(z) \triangleq \boldsymbol{X}^T(z) \left(\boldsymbol{I}_M \otimes \boldsymbol{e}^T(z) \right).
$$

Note that $\boldsymbol{\alpha}$ is the unknown parameters vector to be identified. Equation (4.5) is the basis of the proposed identification algorithm. Next, we will discuss the identification algorithm based on this equation.

4.3 Algorithm Description

Consider an LPTV system with period M mentioned before and assume that the alias components are FIR with L taps. We apply a period-N input signal

$$
\boldsymbol{x} = [x(0), x(1), \cdots, x(N-1)]^T
$$

to this LPTV system, where N is an integer multiple of M, i.e., $N = KM, k \in \mathbb{Z}$. Given the periodic input, the output in the steady-state will be periodic with the same period N. Due to the periodicity of the input and the output, we can take the DFT of the input and the output signals without frequency leakage. Evaluating (4.5) at frequency $\omega_k = 2\pi k/N$ (i.e., $z = W_N^{-k}$) gives

$$
\begin{aligned}
Y[k] &= \boldsymbol{\varphi}^T(W_N^{-k})\boldsymbol{\alpha} + \mathcal{F}\{u(n)\} \\
&= \boldsymbol{\varphi}^T(W_N^{-k})\boldsymbol{\alpha} + w[k],
\end{aligned}
\tag{4.6}
$$

where

$$
Y[k] \triangleq Y(W_N^{-k})
$$

37

are the DFT coefficients of the output $y(n)$, $u(n)$ is assumed to be the i.i.d Gaussian-distributed noise with zero mean and a variance of σ^2 that contaminates the measurements, i.e.,

$$\boldsymbol{u} \sim \mathcal{N}(0, \sigma^2 \boldsymbol{I}_N),$$

$w[k]$ are the DFT coefficients of $u(n)$ and the symbol $\mathcal{F}\{\cdot\}$ denotes DFT operator. Here, we use $\boldsymbol{u}$ to refer to the noise vector and $\boldsymbol{w}$ to refer to the corresponding DFT coefficients vector.

Defining

$$\boldsymbol{\varphi}^T[k] \triangleq \boldsymbol{\varphi}^T(W_N^{-k}),$$

$$\boldsymbol{X}^T[k] \triangleq \boldsymbol{X}^T(W_N^{-k}),$$

and

$$\boldsymbol{e}^T[k] \triangleq \boldsymbol{e}^T(W_N^{-k}),$$

we have

$$
\begin{aligned}
\boldsymbol{X}^T[k] &= \left[X(W_N^{-k}), X(W_N^{-k}W_M^{-1}), \cdots, X\left(W_N^{-k}W_M^{-M+1}\right) \right] \\
&= \left[X(W_N^{-k}), X(W_N^{-k-K}), \cdots, X\left(W_N^{-k-(M-1)K)}\right) \right] \\
&= \left[X[k], X[k+K], \cdots, X\left[k+(M-1)K\right] \right],
\end{aligned}
\tag{4.7}
$$

and

$$
\begin{aligned}
\boldsymbol{\varphi}^T[k] &= \boldsymbol{X}^T(W_N^{-k}) \left(\boldsymbol{I}_M \otimes \boldsymbol{e}^T(W_N^{-k}) \right) \\
&= \boldsymbol{X}^T[k] \left(\boldsymbol{I}_M \otimes \boldsymbol{e}^T[k] \right).
\end{aligned}
\tag{4.8}
$$

Putting all together, equation (4.6) can be rewritten as

$$Y[k] = \boldsymbol{\varphi}^T[k]\boldsymbol{\alpha} + w[k]. \tag{4.9}$$

By stacking the N samples, equation (4.9) can be rearranged in a matrix form as follow

$$\mathcal{Y} = \boldsymbol{\Phi}\boldsymbol{\alpha} + \boldsymbol{w}, \tag{4.10}$$

where

$$\mathcal{Y}^T \triangleq [Y[0], Y[1], \cdots, Y[N-1]],$$

$$\boldsymbol{\Phi}^T \triangleq [\boldsymbol{\varphi}[0], \boldsymbol{\varphi}[1], \cdots, \boldsymbol{\varphi}[N-1]],$$

and

$$\boldsymbol{w}^T \triangleq [w[0], w[1], \cdots, w[N-1]].$$

In the least-squares sense, the unknown vector $\boldsymbol{\alpha}$ can be determined by

$$\hat{\boldsymbol{\alpha}}_{\mathrm{LS}} = \arg \min_{\alpha} \|\mathcal{Y} - \boldsymbol{\Phi}\boldsymbol{\alpha}\|_2^2, \tag{4.11}$$

where $\|\boldsymbol{X}\|_2^2 = \mathrm{tr}\left(\boldsymbol{X}\boldsymbol{X}^H\right)$. If the matrix $\boldsymbol{\Phi}$ is of full column rank (later we will see that the full column rank assumption is trivial if we employ the optimal training signal as the input signal) so that the Gram matrix $\boldsymbol{\Phi}^H\boldsymbol{\Phi}$ is positive definite, then $\hat{\boldsymbol{\alpha}}_{\mathrm{LS}}$ is uniquely determined by

$$\hat{\boldsymbol{\alpha}}_{\mathrm{LS}} = (\boldsymbol{\Phi}^H\boldsymbol{\Phi})^{-1}\boldsymbol{\Phi}^H\mathcal{Y}, \tag{4.12}$$

where $\hat{\boldsymbol{\alpha}}_{\mathrm{LS}}^T = \left[\hat{\boldsymbol{\alpha}}_0^T, \hat{\boldsymbol{\alpha}}_1^T, \cdots, \hat{\boldsymbol{\alpha}}_{L-1}^T\right]$. Here, we assume that N is greater than or equal to ML. If N is less than ML, it is impossible to identify those parameters uniquely. Because the input training signal is known, $[\boldsymbol{\Phi}^H\boldsymbol{\Phi}]^{-1}\boldsymbol{\Phi}^H$ can be precomputed and stored so that the complexity of computation is decreased further. In the next section, we will discuss the performance of this LS estimator and present the design of the optimal training signal.

Remark: In the derivation above, we have assumed that N is a multiple of M. If N is not a multiple of M, the output will be periodic with period $\bar{N}$ equal to the least common multiple of N and M. That is, we need to use $\bar{N}$ sample of the output signal $y(n)$ in one period. In this case, even when the constraint $N = KM, k \in \mathbb{Z}$ is not satisfied, we still can generalize the previous discussion to relate the N-point DFT coefficients of the input and the $\bar{N}$-point DFT coefficients of the output. If $\bar{N}$ is greater than or equal to ML, the proposed algorithm still can be used.

4.4 Performance Analysis and Optimal Training Signal Design

This section investigates the performance of the least-squares estimator for FIR-LPTV systems. An MSE lower bound on the LS estimator is derived and the design of an optimal training signal to achieve this bound is given. For completeness, at the beginning we summarize two main DFT

properties used in this paper. Let

$$X[k] = \sum_{n=0}^{N-1} x(n) W_N^{kn},$$

and

$$x(n) = \sum_{k=0}^{N-1} X[k] W_N^{-kn},$$

i.e., $x(n) \overset{\mathcal{F}}{\longleftrightarrow} X[k]$.

$\underline{\text{Property} - 1}$: $\boldsymbol{F}_N^H \boldsymbol{F}_N = \boldsymbol{F}_N \boldsymbol{F}_N^H = N \boldsymbol{I}_N$, i.e., the columns (rows) of the DFT matrix are orthonormal to each other.

$\underline{\text{Property} - 2}$: $W_N^{ln} x(n) \overset{\mathcal{F}}{\longleftrightarrow} X[(k+l)_N]$, hence representing a cyclically-shifted version. Its duality is given by

$$x[(n+m)_N] \overset{\mathcal{F}}{\longleftrightarrow} W_N^{-mk} X[k].$$

In the following, we will discuss the MSE bound of the proposed least-squares estimator and the optimal training signal design.

4.4.1 MSE Bound of LS Estimator

We will first discuss the relationship of the errors in the coefficients of alias components and the $\mathcal{H}_2$-norm of an error system. Then, we will find some bound of the LS estimator, which in turn will give us some bound on the energy of errors to an impulse input.

In fact, minimizing the square error coefficients of the alias components is equivalent to minimizing the square error of the impulse response in the sense of $\mathcal{H}_2$-norm. Here, we include the proof here. In the following, we will show that minimizing the square error coefficients of the alias components $A_m(z)$ is equivalent to minimizing the square error of the impulse response in the sense of $\mathcal{H}_2$-norm. Take a periodic-M LPTV system $\mathcal{A}$ into consideration. The input x and the output y of the LPTV system can be related by

$$y(k) = \sum_{l=0}^{\infty} g(k, l) x(l), \tag{4.13}$$

where $g(k, l)$ is the response of the system at time k to an impulse applied at time l in its input, i.e., the Green function. Due to the periodic condition on the system, the impulse response has the

property

$$g(k + M, l + M) = g(k, l), \quad \forall k, l. \tag{4.14}$$

An equivalent representation can be obtained by setting $h(l, k) = g(l + k, l)$. The M-periodic property on $\mathcal{A}$ gives

$$h(l, k) = h(l + M, k).$$

Substituting h for g in (4.13) , we get

$$y(k) = \sum_{i=-\infty}^{k} h(i, k - i)x(i).$$

Now, we consider the $\mathcal{H}_2$-norm of the LPTV system $\mathcal{A}$. By applying the impulse $\delta(k - m), 0 \leq m \leq M - 1$ to the input of $\mathcal{A}$, we have the output

$$y_m(k) = h(m, k - m).$$

Thus, the frequency representation of the the ouput w.r.t. $\delta(k - m)$ is

$$
\begin{aligned}
Y_m(z) &= \sum_{k=0}^{\infty} h(m, k - m)z^{-k} \\
&= \sum_{k=0}^{\infty} h(m, k - m)z^{-(k-m+m)} \\
&= z^{-m} \sum_{k=0}^{\infty} h(m, k - m)z^{-(k-m)} \\
&= z^{-m} H_m(z),
\end{aligned}
$$

where $H_m(z) = \sum_{k=0}^{\infty} h(m, k)z^{-k}$ with $H_m(z) = H_{m+M}(z)$. The 2-norm of this output $Y_m(z)$ is equal to $\|H_m(z)\|_2$. Because of the M-periodic property, the $\mathcal{H}_2$-norm of the LPTV system $\mathcal{A}$ is equal to averaging the squares of the 2-norms of the outputs of $\mathcal{A}$ in terms of impulses at time 0 through $M - 1$ [23] in the manuscript, that is,

$$
\begin{aligned}
\|\mathcal{A}\|_2 &= \left(\frac{1}{M} \sum_{m=0}^{M-1} \|H_m(z)\|_2^2 \right)^{1/2} \\
&= \left(\frac{1}{M} \boldsymbol{H}^T(z)\boldsymbol{H}(z) \right)^{1/2},
\end{aligned}
\tag{4.15}
$$

with $\boldsymbol{H} = [H_0(z), H_1(z), \cdots, H_{M-1}(z)]^T$. The relationship between $\boldsymbol{A}(z)$ and $\boldsymbol{H}(z)$ is given by [6] in the manuscript

$$\boldsymbol{H}(z) = \boldsymbol{F}_M \boldsymbol{A}(z). \tag{4.16}$$

41

Substituting (4.16) into (4.15) results in

$$
\begin{aligned}
\|\mathcal{A}\|_2 &= \left(\frac{1}{M} (\boldsymbol{F}_M \boldsymbol{A}(z))^T (\boldsymbol{F}_M \boldsymbol{A}(z)) \right)^{1/2} \\
&= \left(\frac{1}{M} \boldsymbol{A}^T(z) \boldsymbol{A}(z) \right)^{1/2} \\
&= \left(\frac{1}{M} \sum_{m=0}^{M-1} \|A_m(z)\|_2^2 \right)^{1/2} \\
&= \left(\frac{1}{M} \sum_{m=0}^{M-1} \sum_{i=0}^{L-1} \|a_{m,i}\|_2^2 \right)^{1/2}.
\end{aligned}
\tag{4.17}
$$

The mean-square error of the coefficients of the alias components $A_m(z)$ is also equal to the square error of the impulse responses of an LPTV error system. Such an error system is formed by subtracting the estimated system $\hat{\mathcal{A}}$ from the true system $\mathcal{A}$. As the error system is an LPTV system, the square of its $\mathcal{H}_2$-norm can be defined as the average of the squares of the 2-norms of its outputs to impulses at time 0 through $M - 1$ [81]. It can be shown that

$$
\|\mathcal{A} - \hat{\mathcal{A}}\|_2 = \left(\frac{1}{M} \sum_{m=0}^{M-1} \sum_{i=0}^{L-1} \|a_{m,i} - \hat{a}_{m,i}\|_2^2 \right)^{1/2}
\tag{4.18}
$$

$$
= \|\boldsymbol{\alpha} - \hat{\boldsymbol{\alpha}}_{\mathrm{LS}}\|_2.
$$

Thus, minimizing the mean-square error of the coefficients is equivalent to minimizing the $\mathcal{H}_2$-norm of the error system. In the following, we will discuss the bound of the LS estimator.

Using (4.10) and (4.12), we have

$$
\begin{aligned}
\hat{\boldsymbol{\alpha}}_{\mathrm{LS}} &= (\boldsymbol{\Phi}^H \boldsymbol{\Phi})^{-1} \boldsymbol{\Phi}^H (\boldsymbol{\Phi}\boldsymbol{\alpha} + \boldsymbol{w}) \\
&= \boldsymbol{\alpha} + (\boldsymbol{\Phi}^H \boldsymbol{\Phi})^{-1} \boldsymbol{\Phi}^H \boldsymbol{w} \\
&= \boldsymbol{\alpha} + (\boldsymbol{\Phi}^H \boldsymbol{\Phi})^{-1} \boldsymbol{\Phi}^H \boldsymbol{F}_N \boldsymbol{u}.
\end{aligned}
\tag{4.19}
$$

From equation (4.18), we can see that minimizing the square error coefficients of the alias components $A_m(z)$ is equivalent to minimizing the square error of the impulse response $H_m(z)$. Thus, $\hat{\boldsymbol{\alpha}}_{\mathrm{LS}}$ is the sum of the true $\boldsymbol{\alpha}$ and a term induced by the noise. Taking the ensemble average over the left hand side and the right hand side gives

$$
E(\hat{\boldsymbol{\alpha}}_{\mathrm{LS}}) = \boldsymbol{\alpha},
$$

which demonstrates that the proposed estimator is unbiased.

Letting

$$\varepsilon_{\mathrm{LS}} = \hat{\boldsymbol{\alpha}}_{\mathrm{LS}} - \boldsymbol{\alpha} = (\boldsymbol{\Phi}^H \boldsymbol{\Phi})^{-1} \boldsymbol{\Phi}^H \boldsymbol{F}_N \boldsymbol{u},$$

we have the MSE given by

$$\mathrm{MSE} = E(\|\varepsilon_{\mathrm{LS}}\|_2^2)$$

$$= \mathrm{tr}\left(E(\varepsilon_{\mathrm{LS}} \varepsilon_{\mathrm{LS}}^H)\right) \tag{4.20}$$

$$= N\sigma^2 E\left(\mathrm{tr}\left((\boldsymbol{\Phi}^H \boldsymbol{\Phi})^{-1}\right)\right).$$

Before deriving the lower MSE bound for the estimated alias components, we first consider the

term $\mathrm{tr}\left((\boldsymbol{\Phi}^H \boldsymbol{\Phi})^{-1}\right)$. Noticing that $\boldsymbol{\varphi}^T[k]$ can be rewritten as

$$\boldsymbol{\varphi}^T[k] = \boldsymbol{X}^T[k]\left(\boldsymbol{I}_M \otimes \boldsymbol{e}^T[k]\right)$$

$$= \left(X[k]\boldsymbol{e}^T[k], \cdots, X\left[k + (M-1)K\right]\boldsymbol{e}^T[k]\right),$$

we can write the matrix $\boldsymbol{\Phi}$ as following

$$\boldsymbol{\Phi} = \begin{bmatrix} X[0]\boldsymbol{e}^T[0] & \cdots & X[(M-1)K]\boldsymbol{e}^T[0] \\ X[1]\boldsymbol{e}^T[1] & \cdots & X[1+(M-1)K]\boldsymbol{e}^T[1] \\ \vdots & \ddots & \vdots \\ X[N-1]\boldsymbol{e}^T[N-1] & \cdots & X[(M-1)K-1]\boldsymbol{e}^T[N-1] \end{bmatrix}.$$

Here, there are ML columns of the matrix $\boldsymbol{\Phi}$. We formulate the $(mL+l)$th $(m = 0, 1, \cdots, M-1; l =$

$0, 1, \cdots, L-1)$ column vector of this matrix as following

$$\boldsymbol{\psi}_{m,l} = \Lambda^l \boldsymbol{F}_N \Lambda^{mK} \boldsymbol{x}, \tag{4.21}$$

where we have used property-2 and

$$\Lambda \triangleq \mathrm{diag}\left(1, W_N^1, \cdots, W_N^{N-1}\right)$$

is a diagonal matrix with its kth diagonal element as W_N^{k-1}.

We assume that the periodic-N input signal has a constant power, i.e.,

$$\|\boldsymbol{x}\|_2^2 = E_{av}$$

where E_{av} is a constant. Consider the diagonal element of the Gram matrix $\boldsymbol{\Phi}^H \boldsymbol{\Phi}$. Using (4.21),

we have

$$\boldsymbol{\psi}_{m,l}^H \boldsymbol{\psi}_{m,l} = N E_{av} \tag{4.22}$$

43

where

$$0 \leq m \leq M - 1,$$

and

$$0 \leq m \leq L - 1.$$

This equation indicates that the diagonal elements of $\mathbf{\Phi}^H \mathbf{\Phi}$ are constants once the input training signal $\boldsymbol{x}$ is fixed. Let $\lambda_1, \lambda_2, \cdots, \lambda_{ML}$ be the eigenvalues of $\mathbf{\Phi}^H \mathbf{\Phi}$. Then, we have

$$\mathrm{tr}(\mathbf{\Phi}^H \mathbf{\Phi}) = \lambda_1 + \lambda_2 + \cdots + \lambda_{ML} = NMLE_{av}.$$

Note that

$$\mathrm{tr}((\mathbf{\Phi}^H \mathbf{\Phi})^{-1}) = \lambda_1^{-1} + \lambda_2^{-1} + \cdots + \lambda_{ML}^{-1}.$$

Hence, finding the lower bound of MSE is equivalent to finding the solution to the following optimization problem [82]

$$
\begin{aligned}
\text{minimize} \quad & \lambda_1^{-1} + \lambda_2^{-1} + \cdots + \lambda_{ML}^{-1} \\
\text{subject to} \quad & \lambda_1 + \lambda_2 + \cdots + \lambda_{ML} = NMLE_{av}.
\end{aligned}
\tag{4.23}
$$

Given the matrix $\mathbf{\Phi}^H \mathbf{\Phi}$ is positive definite, the minimum MSE (MMSE) is achieved if and only if

$$\lambda_1 = \lambda_2 = \cdots = \lambda_{ML} = NE_{av}. \tag{4.24}$$

The above equation is satisfied when

$$\mathbf{\Phi}^H \mathbf{\Phi} = NE_{av} \boldsymbol{I}_{ML}, \tag{4.25}$$

and the corresponding MMSE is

$$\mathrm{MMSE} = N\sigma^2 \times \frac{ML}{NE_{av}} = \frac{ML\sigma^2}{E_{av}}. \tag{4.26}$$

4.4.2 Optimal Training Signal Design

In this subsection, we will investigate the design of the optimal training signal which achieves the lower MSE bound in equation (4.26). For LTI systems identification, the pseudo-random noise is

the optimal training signal as mentioned in [75], while we will see that the pseudo-random noise is not the optimal training signal for LPTV systems.

In order to achieve the MSE bound, we need to consider the following condition from (4.25):

$$\boldsymbol{\psi}_{m,l}^{H}\boldsymbol{\psi}_{m',l'} = 0 \quad \forall (m - m')L + l - l' \neq 0, \tag{4.27}$$

where

$$m, m' \in \{0, \cdots, M - 1\},$$

and

$$l, l' \in \{0, \cdots, L - 1\}.$$

Using equation (4.21), the following condition is obtained from (4.27)

$$\begin{aligned}
\boldsymbol{\psi}_{m,l}^{H}\boldsymbol{\psi}_{m',l'} &= (\Lambda^{l}\boldsymbol{F}_{N}\Lambda^{mK}\boldsymbol{x})^{H}(\Lambda^{l'}\boldsymbol{F}_{N}\Lambda^{m'K}\boldsymbol{x}) \\
&= \boldsymbol{x}^{H}\Lambda^{-mK}\boldsymbol{F}_{N}^{H}\Lambda^{l'-l}\boldsymbol{F}_{N}\Lambda^{m'K}\boldsymbol{x} \\
&= \boldsymbol{x}^{H}\Pi_{m,m'}^{(d)}\boldsymbol{x} \\
&= 0,
\end{aligned} \tag{4.28}$$

where

$$\Pi_{m,m'}^{(d)} \triangleq \Lambda^{-mK}\boldsymbol{F}_{N}^{H}\Lambda^{d}\boldsymbol{F}_{N}\Lambda^{m'K},$$

and

$$d \in \{-L + 1, \cdots, -1, 0, 1, \cdots, L - 1\}.$$

Note that the (i, j)th element of the matrix $\Pi_{m,m'}^{(d)}$ can be written as

$$\left[\Pi_{m,m'}^{(d)}\right]_{ij} = W_{N}^{-imK+jm'K}\left(\sum_{k=0}^{N-1} W_{N}^{k(j-i+d)}\right). \tag{4.29}$$

Using the identity

$$\sum_{p=0}^{N-1} W_{N}^{pq} = 0 \quad (q \text{ not an integer multiple of } N),$$

we can reformulate (4.29) as

$$\left[\Pi_{m,m'}^{(d)}\right]_{ij} = \begin{cases} NW_{N}^{-imK+jm'K}, & (j - i + d) \text{ is a multiple of } N \\ 0, & \text{otherwise.} \end{cases} \tag{4.30}$$

45

Furthermore, letting $j - i + d = pN, p \in \mathbb{Z}$ and substituting it into (4.30) gives

$$W_N^{-imK+jm'K} = W_N^{-imK+(i-d+pN)m'K}$$

$$= W_N^{-dm'K} \times W_N^{i\Delta K}.$$

Thus

$$\left[\Pi_{m,m'}^{(d)}\right]_{ij} = \begin{cases} W_N^{-dm'K} \times W_N^{i\Delta K}, & (i-j)_N = d \\ 0, & \text{otherwise.} \end{cases} \tag{4.31}$$

where

$$\Delta \triangleq m' - m,$$

and hence

$$\Delta \in \{-M+1, \cdots, 0, \cdots, M-1\}.$$

Now, we recall condition (4.25) for convenience

$$\boldsymbol{x}^H \Pi_{m,m'}^{(d)} \boldsymbol{x} = \begin{cases} NE_{av}, & \Delta = d = 0 \\ 0, & \text{otherwise.} \end{cases} \tag{4.32}$$

Note that condition (4.28) is subsumed in (4.32). Because $\boldsymbol{x}^H \Pi_{m,m'}^{(d)} \boldsymbol{x} \equiv NE_{av}$ always holds when $\Delta = d = 0$, we only need to choose the training signal to make $\boldsymbol{x}^H \Pi_{m,m'}^{(d)} \boldsymbol{x} = 0$ when $\Delta^2 + d^2 \neq 0$. Substituting (4.31) into (4.32), we can rewrite (4.32) in a sum form

$$\boldsymbol{x}^H \Pi_{m,m'}^{(d)} \boldsymbol{x} = \sum_{i=0}^{N-1} \sum_{j=0}^{N-1} x^*(i) \left[\Pi_{m,m'}^{(d)}\right]_{ij} x(j)$$

$$= W_N^{-dm'K} \times \left(\sum_{i=0}^{N-1} x^*(i) W_N^{i\Delta K} x((i-d)_N)\right)$$

$$= 0$$

that is

$$\sum_{i=0}^{N-1} W_N^{i\Delta K} x^*(i) x\left((i-d)_N\right) = 0, \tag{4.33}$$

where

$$\Delta \in \{-M+1, \cdots, 0, \cdots, M-1\},$$

and

$$d \in \{-L+1, \cdots, -1, 0, 1, \cdots, L-1\}.$$

Considering the circularity of W_N, the modular operation and the assumption $N = MK$, we have at most $ML - 1$ distinct non-trivial equations in (4.33). ($\Delta = d = 0$ is considered as the trivial case.) We rewrite (4.33) in the following

$$
\begin{cases}
\displaystyle\sum_{i=0}^{N-1} W_N^{i\Delta K} x^*(i) x\left((i - d)_N\right) = 0 \\[2ex]
\Delta \in \{0, 1, \cdots, M - 1\} \\[1ex]
d \in \{0, 1, \cdots, L - 1\} \\[1ex]
\Delta^2 + d^2 \neq 0.
\end{cases}
\tag{4.34}
$$

Note that in the above, repeated equations were eliminated.

Next, let us consider LTI systems first. In (4.34), we have $M = 1$, which results in $\Delta = 0$. Thus, the optimal input satisfies

$$
\sum_{i=0}^{N-1} x^*(i) x\left((i - d)_N\right) = 0, \ \forall d \in \{1, \cdots, L - 1\}.
$$

That is, pseudo-randomly generated inputs are optimal for LTI systems. However, for LPTV systems pseudo-randomly generated inputs do not necessarily satisfy equation set (4.34). That is, pseudo-random signals are not the optimal training signals for LPTV systems, even if they are the optimal training signals for LTI systems.

For LPTV systems, in order to find the optimal input, we need to solve equation set (4.34). This is a set of multivariate quadratic polynomial equations. Similar equations arise in the design of public key cryptographic systems. These equations are NP-complete [83], and generally difficult to solve. It is hard to get an analytic solution, but it may be possible to develop a method similar to that given in [84] to test whether there exists a nontrivial solution to the equation set (4.34). At the same time, we can adjust the period of the input signal N so that an underdetermined system is formed and an optimal training signal exists. For example, if for a specified N there is no optimal training signal, we can increase N to achieve the optimal training signal. Generally, if the number of the parameters to be estimated is small, the equation set can be solved by hand. Note that if the optimal training signal is applied, the Gram matrix $\mathbf{\Phi}^H \mathbf{\Phi}$ will be diagonal and can be easily inverted.

4.5　Extension to IIR-LPTV Systems

In this section, we extend the proposed algorithm to IIR-LPTV systems. The parts that are similar to the discussion in the previous sections on the FIR case will be discussed briefly and the main emphasis will be on the extension to the IIR case. In particular, variables that were defined in previous sections will remain unchanged. Without loss of generality, we assume that all of the branches have the same denominator:

$$
\begin{aligned}
A_m(z) &= \frac{\displaystyle\sum_{i=0}^{L_n-1} a_{m,i} z^{-i}}{1 + \displaystyle\sum_{i=1}^{L_d-1} b_i z^{-i}} \\
&= \frac{\boldsymbol{\alpha}_m^T \boldsymbol{e}(z)}{1 + \boldsymbol{\beta}^T \boldsymbol{e}_d(z)},
\end{aligned}
$$

where L_n and L_d are the order of the numerator and the denominator, respectively, with

$$
\boldsymbol{e}_d(z) = [z^{-1}, \cdots, z^{-(L_d-1)}]^T,
$$

and

$$
\boldsymbol{\beta} \triangleq [\beta_1, \beta_2, \cdots, \beta_{L_d-1}]^T.
$$

The relationship between the input x and the output y is

$$
\begin{aligned}
Y(z) &= \boldsymbol{X}^T(z) \left[A_0(z), \cdots, A_{M-1}(z)\right]^T \\
&= \frac{\boldsymbol{X}^T(z) \left[\boldsymbol{\alpha}_0^T \boldsymbol{e}(z), \cdots, \boldsymbol{\alpha}_{M-1}^T \boldsymbol{e}(z)\right]^T}{1 + \boldsymbol{\beta}^T \boldsymbol{e}_d(z)} \\
&= \frac{\boldsymbol{X}^T(z)(\boldsymbol{I}_M \otimes \boldsymbol{e}^T(z))\boldsymbol{\alpha}}{1 + \boldsymbol{\beta}^T \boldsymbol{e}_d(z)} \\
&= \frac{\boldsymbol{\varphi}^T(z)\boldsymbol{\alpha}}{1 + \boldsymbol{\beta}^T \boldsymbol{e}_d(z)}.
\end{aligned}
\tag{4.35}
$$

Simplifying (4.35) gives

$$
Y(z)(1 + \boldsymbol{\beta}^T \boldsymbol{e}_d(z)) = \boldsymbol{\varphi}^T(z)\boldsymbol{\alpha},
$$

which is equivalent to

$$
Y(z) = \left[\boldsymbol{\varphi}^T(z), -Y(z)\boldsymbol{e}_d^T(z)\right] \begin{bmatrix} \boldsymbol{\alpha} \\ \boldsymbol{\beta} \end{bmatrix}.
\tag{4.36}
$$

Applying the same method for FIR-LPTV systems in Section 4.3, we have

$$Y[k] = \left[\boldsymbol{\varphi}^T[k], -Y[k]\boldsymbol{e}_d^T[k]\right] \begin{bmatrix} \boldsymbol{\alpha} \\ \boldsymbol{\beta} \end{bmatrix} \tag{4.37}$$

with

$$\boldsymbol{e}_d^T[k] \triangleq \boldsymbol{e}_d^T(W_N^{-k}).$$

Stacking the N samples in one period, we have the matrix form of equation (4.37)

$$\mathcal{Y} = \boldsymbol{\Psi} \begin{bmatrix} \boldsymbol{\alpha} \\ \boldsymbol{\beta} \end{bmatrix},$$

with

$$\mathcal{Y} = \begin{bmatrix} Y[0] \\ \vdots \\ Y[N-1] \end{bmatrix}, \quad \boldsymbol{\Psi} = \begin{bmatrix} \boldsymbol{\varphi}^T[0] & -Y[0]\boldsymbol{e}_d^T[0] \\ \vdots & \vdots \\ \boldsymbol{\varphi}^T[N-1] & -Y[N-1]\boldsymbol{e}_d^T[N-1] \end{bmatrix}.$$

Using the least-squares method, we have the estimated parameters

$$\begin{bmatrix} \hat{\boldsymbol{\alpha}} \\ \hat{\boldsymbol{\beta}} \end{bmatrix}_{\text{LS}} = (\boldsymbol{\Psi}^H \boldsymbol{\Psi})^{-1} \boldsymbol{\Psi}^H \mathcal{Y}.$$

Here, we assume that the period of the input signal N is greater than the number of unknown parameters $ML_n + L_d - 1$, and $\boldsymbol{\Psi}^H \boldsymbol{\Psi}$ is of full rank. Note that contrary to the FIR case, it is not straightforward to relate the error in the approximation of coefficients and the $\mathcal{H}_2$ norm of the error system. Moreover, we were not able to extend the results for optimal signal design, to the IIR case.

4.6 Numerical Results

In this section, the performance of the proposed method is illustrated by numerical simulations. Both FIR-LPTV and IIR-LPTV systems identification algorithms are examined.

4.6.1 FIR-LPTV Examples with Optimal Input

Take an FIR-LPTV system with period $M = 2$. The corresponding frequency response of each branch is given in Table 4.1.

Table 4.1: Alias Components for an FIR-LPTV System

$A_0(z)$	$0.7 + 0.05z^{-1} + 0.04z^{-2} + 2.05z^{-3}$
$A_1(z)$	$-0.1 + 0.15z^{-1} + 0.06z^{-2} + 0.45z^{-3}$
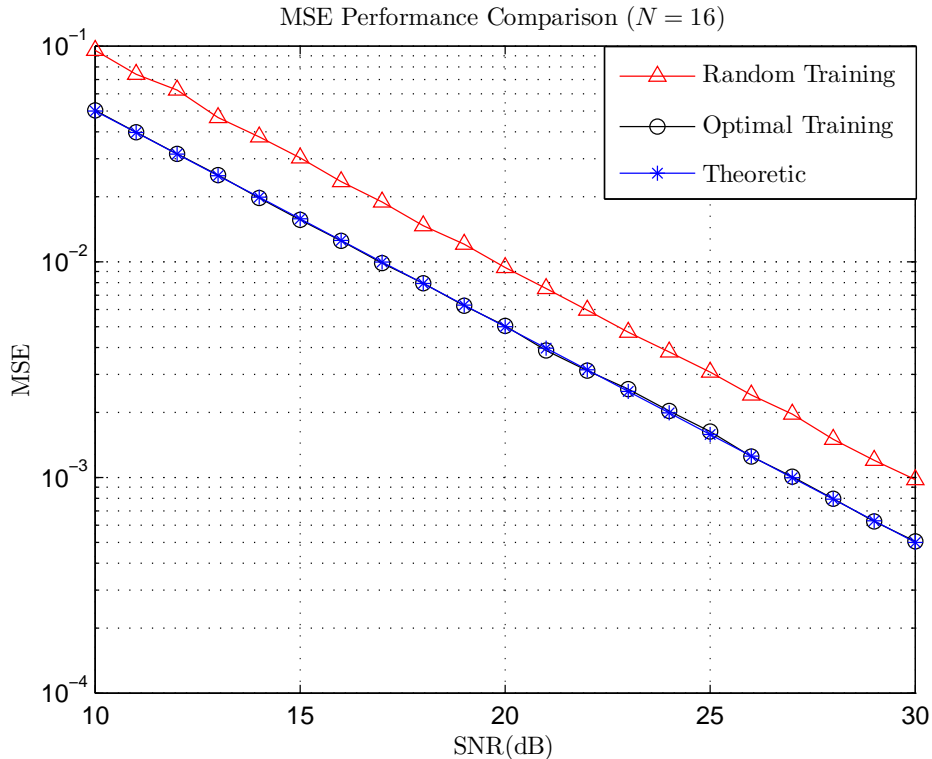
Figure 4.2: MSE curve for the FIR-LPTV system.

Here, we choose $N = 16 > ML = 8$. Based on equation (4.33), one possible optimal training signal is $\frac{\sqrt{2}}{2}[1, -3, 1, 1, 1, 1, 1, 1, 1, 1, -3, 1, 1, 1, 1, 1]$, where the constant $\frac{\sqrt{2}}{2}$ is used to normalize the input signal so that the average power is equal to 1. In order to compare the results, we have also used a randomly generated periodic-N input signal.

Gaussian noise is added to the output. We change the signal to noise ratio (SNR) and perform Monte-Carlo simulations. Figure 4.2 gives the simulation results. Those ensemble average MSE curves are generated by using MATLAB after 40 trials. Here, we can see that the theoretic MSE curve agrees with the MSE curve under the optimal training signal, while the pseudo-random input signal is about 4 dB worse. This demonstrates that the design of the optimal training signal can
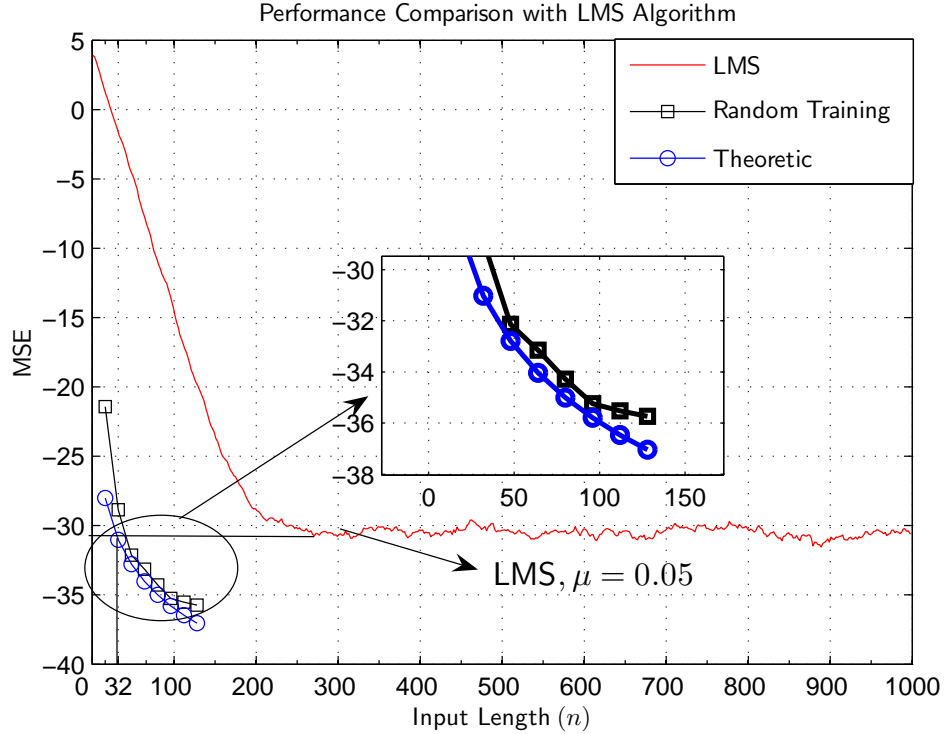
Figure 4.3: Performance comparison of the given method with the LMS algorithm.

improve the identification accuracy. It also shows that short pseudo-random input signals are not optimal for the identification of LPTV systems. Furthermore, the optimal training signals will lead to diagonal Gram matrices that can be easily inverted; however for random training signals the Gram matrix $\boldsymbol{\Phi}^H\boldsymbol{\Phi}$ is not necessarily a diagonal matrix. Here, we also find that the SNR vs the MSE is straight line. At the first glance, it seems not reasonable. However, when looking into equation (4.20), it is found that the last term $E\left(\mathrm{tr}\left((\boldsymbol{\Phi}^H\boldsymbol{\Phi})^{-1}\right)\right)$ is actually a constant. Then, the noise variance is linearly proportionate to the MSE. That's why the SNR vs MSE curve figure is a linear curve.

A comparison with the LMS algorithm [58] is presented in Figure 4.3. From this figure, we can see that the proposed method outperforms the LMS algorithm. In order to get an MSE equal to 30 dB, using our method, we need a training signal of length 32. However, using the LMS algorithm, comparable errors are obtained when the input signal length is greater than 250. Once the optimal training signal is used, the computational complexity is reduced considerably. As we mentioned before, the Gram matrix has full column rank. Therefore, the identification method is not only

more accurate but also more efficient than the LMS algorithm when the optimal training signal is applied. From Figure 4.3, we also see that the performance of the random training signal will approach that of the optimal training signal as the length of the input signal increases. Therefore, from a practical point of view, the optimal training signal is desirable mainly when the length of the training signal is short.

4.6.2 Time Domain Algorithms for FIR-LPTV

As mentioned in the Section 4.1, the algorithm can be derived in the time domain, in which case, an LSTV setup can be used to derive the algorithm in the time domain [6] in the manuscript. Figure 4.4 shows the simulation results of the time domain algorithm. The MSE curve are generated by performing 1000 trials. We tried different parameters as well. The parameters are given in Table 4.2. According to the simulations, the time domain algorithm gives slightly worse results.

**Table 4.2:** Parameters of Alias Components

$A_0(z)$	$0.7 + 0.05z^{-1} + 0.04z^{-2} + 2.05z^{-3}$
$A_1(z)$	$-0.1 + 0.15z^{-1} + 0.06z^{-2} + 0.45z^{-3}$

However, we should note that in the time domain representation the signal does not have to be periodic. Therefore, the two methods are not exactly equivalent. The constraint $N = KM, K \in \mathbb{Z}$ can be relaxed as we mentioned (given as a remark) in Section 3. The periods of the input and the output signals do not need to be the same. All that is needed is to have the data for a whole period of the output signal of the system. For example, if the period of the input signal $x(n)$ is 5 and the period of the LPTV system is 3, the period of the output $y(n)$ will be 15.

4.6.3 Examples for the Extension to IIR-LPTV

In this example, the setup is the same as the above example for FIR-LPTV systems. The alias components are given in Table 4.3.

We have used the algorithm described in Section 4.5. Figure 4.5 shows the identification results
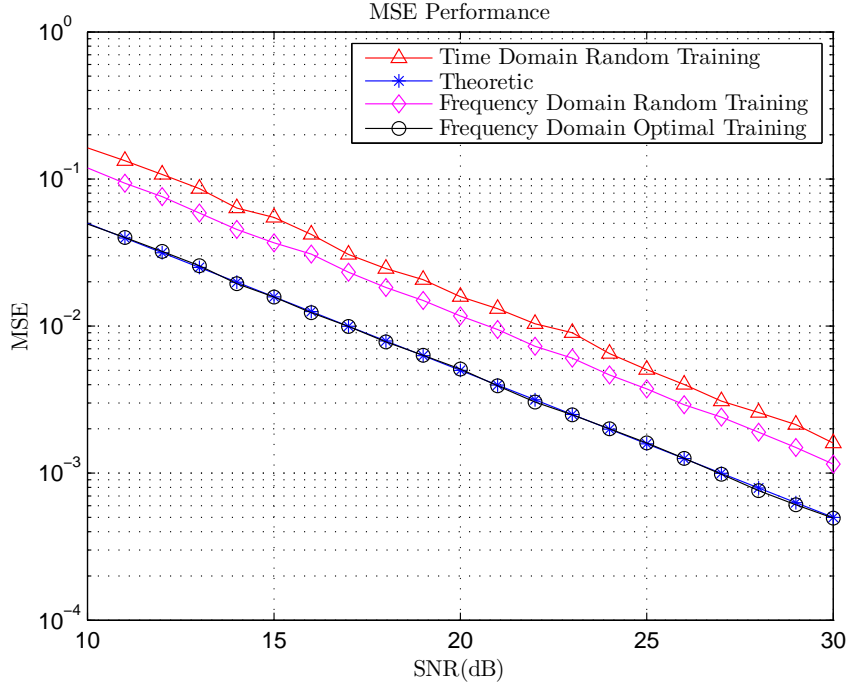
Figure 4.4: MSE curve for the FIR-LPTV system in the time and frequency domain.

Table 4.3: Alias Components for an IIR-LPTV System

$A_0(z)$	$\frac{0.7+0.05z^{-1}+0.04z^{-2}+2.05z^{-3}}{1-1.25z^{-1}+0.33z^{-2}+0.15z^{-3}-0.05z^{-3}}$
$A_1(z)$	$\frac{-0.1+0.15z^{-1}+0.06z^{-2}+0.45z^{-3}}{1-1.25z^{-1}+0.33z^{-2}+0.15z^{-3}-0.05z^{-3}}$

of the above system, when the input signal is randomly generated. As the period of the input signal increases, the MSE curve decrease as expected. Moreover, this example shows that an improvement of about 6dB is obtained if we use an input sequence of length 24, rather than an input sequence of length 16.

4.7   Conclusion

We derived an alias component identification method for FIR based LPTV systems. When a periodic input is applied to an LPTV system and the period of this input

is a multiple of that of the LPTV system, it has shown that the identification method is reduced
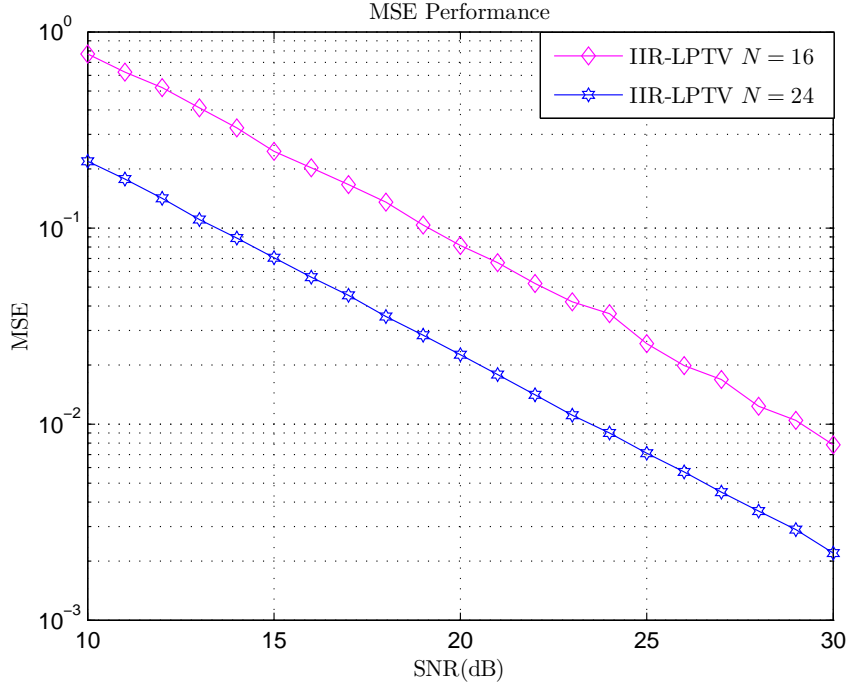
Figure 4.5: MSE curve for the IIR-LPTV system

to solving a least-squares problem in the frequency domain. This method can be generalized to the case when the period of the input is not a multiple of that of the LPTV system. To evaluate the performance of this LS estimator, we derived the lower MSE bound. Simulation results corroborated that the optimal training signal design achieves this lower MSE bound. We also came to the conclusion that the estimation accuracy was increased when compared to the random training signal. We showed that a pseudo-random input signal is not optimal for LPTV systems even if it is the optimal signal for LTI systems. We also extended the algorithm to IIR-LPTV systems. Simulation results showed the accuracy of the estimation, and demonstrated that the performance decreases when a pseudo-random input signal is applied. From the simulation results, we also saw that the optimal training design is advantageous for short training signals. Otherwise, longer pseudo-random input signals are approximately optimal.

CHAPTER 5

CONCLUSIONS AND FUTURE WORK

5.1 Conclusions

This thesis explored the identification of discrete LPTV systems. Using different settings of LPTV systems, we developed two identification algorithms by using periodic inputs. Due to the periodic inputs, the DFT can be used to related the input signal to the output signal in the frequency domain. Because of this favorable characteristic, we used the LS method to identify the coefficients of the LSTV representation and the alias components. In the mean time, an optimal input signal design was considered naturally.

In Chapter 2, we reviewed the basic theory of LPTV systems and its various representations. Difference equations, Green function, LSTV, alias components, MIMO-LTI, and maximally decimated filter banks representations have been fully discussed as each representation can reveal certain aspect of an LPTV system. Based on different representations, different identification algorithms could be developed. These different representations formed the basis of the following chapters, and also acted as a tutorial.

In Chapter 3, we developed an identification method for discrete single-input single-output (SISO) LPTV systems. By using an LSTV structure, we applied a periodic input to the system. We showed that when the period of the input singal is greater than the number of the parameters to be estimated, an overdetermined system is formed and our identification method reduces to finding the LS solution of a set of linear equations. Then, a sufficient condition for identifiability was derived based on a multirate filter bank structure. It is straightforward to generalize this method to MIMO LPTV systems. Simulation results illustrated the accuracy of the proposed method. A

comparison with the LMS algorithms was presented as well.

In Chapter 4, we derived an alias component identification method for FIR based LPTV systems. When a periodic input is applied to an LPTV system and the period of this input is a multiple of that of the LPTV system, it was shown that the identification method is reduced to solving a least-squares problem in the frequency domain. To evaluate the performance of this LS estimator, we derived a lower MSE bound. We showed that a pseudo-random input signal is not optimal for LPTV systems even if it is the optimal signal for LTI systems. We designed optimal training signal to achieve the lower MSE bound. Simulation results showed the accuracy of the proposed method. From the simulation results, we saw that the optimal training design is advantageous for short training signals.

In Chapter 5, a brief conclusion of the thesis was given and the sketch of the future research plan is described.

5.2   Future Work

Our research has so far discussed two identification methods and achieved meaningful results. The exploration is still at its initial stage whereas LPTV system research is a vast world with many areas worth further studying. It is believed that the challenges addressed in this thesis need to be examined in future research.

We observe that Chapter 3 considered only FIR-LPTV systems. In fact, the algorithm can also be generalized to IIR-LPTV systems if all of the branches shared the same denominators. At the same time, we only obtain a necessary condition for the identifiability. In fact, this could lead to the longer sequence than needs. However, due to the high complexity, we can not find the sufficient and necessary condition for the identifiability. Therefore, the sufficient condition still needs to be investigated.

Chapter 4 discussed identification of an LPTV systems by resorting to the alias components representation. Fortunately, we have already generalized the algorithm to the IIR-LPTV case. But we did not find the optimal training sequence for the IIR-LPTV case. Because the optimal inputs

can guarantee the algorithm to achieve the MMSE, it is very meaningful to design. Meanwhile, using the optimal inputs can also reduce the computational complexity. Therefore, it is worth spending some effort designing such kind of optimal inputs in order to achieve the lower MSE bound.

Besides, we believe that using a state-space model to represent IIR-LPTV systems would bring the identification problem much convenience. If a state-space model is used, many control techniques can be modified to identify IIR-LPTV systems such as subspace identification method. Therefore, Other adaptive filtering methods like Kalman filtering can also be used to identify IIR-LPTV systems. Under the framework of control theory, observability and controllability of an IIR-LPTV system can be further discussed.

REFERENCES

[1] T. Chen and L. Qiu, "Linear periodically time-varying discrete-time systems: aliasing and LTI approximations," *Syst. Contr. Lett.*, vol. 30, pp. 225–235, 1997.

[2] G. Gelli and F. Verde, "Blind FSR-LPTV equalization and interference rejection," *IEEE Trans. Communications*, vol. 51, pp. 145–150, 2003.

[3] A. Saadat Mehr and T. Chen, "On alias-component matrices of discrete-time linear periodically time-varying systems," *IEEE Signal Processing Letters*, vol. 8, pp. 114–116, 2001.

[4] F. J. Harris, *Multirate Signal Processing for Communication Systems*. Prentice Hall, 2004.

[5] K. Rajawat, T. Wang, and G. B. Giannakis, "An algebraic polyphase approach to wireless network coding," in *Proc. IEEE International Conference on Acoustics, Speech and Signal Processing ICASSP 2009*, 19–24 April 2009, pp. 2441–2444.

[6] K.-H. Kim, H.-B. Lee, Y.-H. Kim, and S.-C. Kim, "Channel adaptation for time-varying power-line channel and noise synchronized with AC cycle," in *Proc. IEEE International Symposium on Power Line Communications and Its Applications ISPLC 2009*, March 29 2009–April 1 2009, pp. 250–254.

[7] G. Gelli and F. Verde, "Blind LPTV joint equalization and interference suppression," in *Proc. IEEE International Conference on Acoustics, Speech, and Signal Processing ICASSP '00*, vol. 5, 5–9 June 2000, pp. 2753–2756.

[8] H. Zhang, D. Le Ruyet, and M. Terre, "Signal detection for OFDM/OQAM system using cyclostationary signatures," in *Proc. IEEE 19th International Symposium on Personal, Indoor and Mobile Radio Communications PIMRC 2008*, 15–18 Sept. 2008, pp. 1–5.

[9] R. Gandhi and S. K. Mitra, "Aliasing cancelation in block filters and periodically time varying systems: a time-domain approach," in *Proc. IEEE International Symposium on Circuits and Systems ISCAS '97*, vol. 4, June 1997, pp. 2421–2424.

[10] P. P. Vaidyanathan and S. K. Mitra, "Polyphase networks, block digital filtering, LPTV systems, and alias-free qmf banks: a unified approach based on pseudocirculants," *IEEE Transactions on Acoustics, Speech and Signal Processing*, vol. 36, no. 3, pp. 381–391, March 1988.

[11] F. Yuan, "On the periodicity of network functions of periodically switched linear and nonlinear circuits," in *Proc. Canadian Conference on Electrical and Computer Engineering*, vol. 1, March 2000, pp. 574–577.

[12] F. J. Canete, J. A. Cortes, L. Diez, J. T. Entrambasaguas, and J. L. Carmona, "Fundamentals of the cyclic short-time variation of indoor power-line channels," in *Proc. International Symposium on Power Line Communications and Its Applications*, April 2005, pp. 157–161.

[13] M. W. Cantoni and K. Glover, "Robustness of linear periodically-time-varying closed-loop systems," in *Proc. 37th IEEE Conference on Decision and Control*, vol. 4, Dec. 1998, pp. 3807–3812.

[14] X. Chen, C. Zhang, and J. Zhang, "A state space approach to the inverse of LPTV filters," in *Proc. IEEE International Conference on Acoustics, Speech and Signal Processing ICASSP 2006*, vol. 3, 14–19 May 2006, pp. 632–635.

[15] P. Vanassche, G. Gielen, and W. Sansen, "Symbolic modeling of periodically time-varying systems using harmonic transfer matrices," *IEEE Transactions on Computer-Aided Design of Integrated Circuits and Systems*, vol. 21, no. 9, pp. 1011–1024, Sept. 2002.

[16] J. Lerdworatawee and W. Namgoong, "Generalized linear periodic time-varying analysis for noise reduction in an active mixer," *IEEE Journal of Solid-State Circuits*, vol. 42, no. 6, pp. 1339–1351, June 2007.

[17] S. Mirabbasi, B. Francis, and T. Chen, "Input-output gains of linear periodic discrete-time systems with application to multirate signal processing," in *Proc. IEEE International Symposium on Circuits and Systems ISCAS '96., 'Connecting the World'*, vol. 2, 12–15 May 1996, pp. 193–196.

[18] J. Roychowdhury, "Reduced-order modeling of time-varying systems," *IEEE Transactions on Circuits and Systems II: Analog and Digital Signal Processing*, vol. 46, no. 10, pp. 1273–1288, Oct. 1999.

[19] A. Saadat Mehr, "Alias-component matrices of multirate systems," *IEEE Transactions on Circuits and Systems II: Express Briefs*, vol. 56, no. 6, pp. 489–493, June 2009.

[20] M. Vetterli, "Invertibility of linear periodically time-varying filters," *IEEE Transactions on Circuits and Systems*, vol. 36, no. 1, pp. 148–150, Jan. 1989.

[21] G. B. Giannakis, G. Zhou, and M. K. Tsatanis, "On blind channel estimation with periodic misses and equalization of periodically varying channels," in *Conference Record of The Twenty-Sixth Asilomar Conference on Signals, Systems and Computers*, 26–28 Oct. 1992, pp. 531–535.

[22] J. Zhang and C. Zhang, "Robustness of discrete periodically time varying control under different model perturbations," in *Proc. 35th IEEE Decision and Control*, vol. 4, 11–13 Dec. 1996, pp. 3984–3989.

[23] S. Zbigniew, "Power system properties periodical time variance investigations: hardware and software tools development," in *Proc. IEEE Instrumentation and Measurement Technology*, 1–3 May 2007, pp. 1–5.

[24] V. Martin, M. Chabert, and B. Lacaze, "Digital watermarking of natural images based on LPTV filters," in *Proc. IEEE International Conference on Acoustics, Speech and Signal Processing ICASSP 2007*, vol. 2, April 2007, pp. 197–200.

[25] E. Gad and M. Nakhla, "Efficient model reduction of linear periodically time-varying systems via compressed transient system function," *IEEE Transactions on Circuits and Systems I: Regular Papers*, vol. 52, no. 6, pp. 1188–1204, June 2005.

[26] Y. Wan and J. Roychowdhury, "Operator-based model-order reduction of linear periodically time-varying systems," in *Proc. 42nd Design Automation Conference*, 13–17 June 2005, pp. 391–396.

[27] F. J. C. Corripio, J. A. C. Arrabal, L. D. del Rio, and J. T. E. Munoz, "Analysis of the cyclic short-term variation of indoor power line channels," *IEEE Journal on Selected Areas in Communications*, vol. 24, no. 7, pp. 1327–1338, July 2006.

[28] Y. Shi, F. Ding, and T. Chen, "Multirate crosstalk identification in xDSL systems," *IEEE Transactions on Communications*, vol. 54, no. 10, pp. 1878–1886, Oct. 2006.

[29] R. Meyer and C. Burrus, "A unified analysis of multirate and periodically time-varying digital filters," *IEEE Transactions on Circuits and Systems*, vol. 22, no. 3, pp. 162–168, Mar 1975.

[30] T. Chen, L. Qiu, and E.-W. Bai, "General multirate building structures with application to nonuniform filter banks," *IEEE Transactions on Circuits and Systems II: Analog and Digital Signal Processing*, vol. 45, no. 8, pp. 948–958, Aug. 1998.

[31] X. Chen, C. Zhang, and J. Zhang, "Decomposition and noncausal realization of unstable LPTV system," in *Proc. 9th International Conference on Control, Automation, Robotics and Vision ICARCV '06*, 5–8 Dec. 2006, pp. 1–6.

[32] J. J. Yame and R. Hanus, "On stabilization and spectrum assignment in periodically time-varying continuous-time systems," *IEEE Transactions on Automatic Control*, vol. 46, no. 6, pp. 979–983, June 2001.

[33] T. Hagiwara and H. Umeda, "Robust stability analysis of sampled-data systems with noncausal periodically time-varying scaling: Optimization of scaling via approximate discretization and error bound analysis," in *Proc. 46th IEEE Conference on Decision and Control*, 12–14 Dec. 2007, pp. 450–457.

[34] T. Hagiwara and R. Mori, "Robust stability analysis of sampled-data systems via periodically time-varying scaling," in *Proc. American Control Conference*, June 2006, pp. 213–219.

[35] Y. Tange and K. Tsumura, "Periodically weighted model-matching problems by LPTV controllers formulated in dual lifted forms," in *Proc. American Control Conference the 2004*, vol. 4, 30 June–2 July 2004, pp. 3502–3507.

[36] S. Akkarakaran and P. P. Vaidyanathan, "Bifrequency and bispectrum maps: a new look at multirate systems with stochastic inputs," *IEEE Transactions on Signal Processing*, vol. 48, no. 3, pp. 723–736, March 2000.

[37] Y. Tange, "State space parameterization of stabilizing multirate controllers for MIMO linear time-invariant plants," in *Proc. the 44th IEEE Conference on Decision and Control, and the European Control Conference 2005*, Dec. 2005, pp. 1583–1588.

[38] R. Garcia, L. Diez, J. A. Cortes, and F. J. Canete, "Mitigation of cyclic short-time noise in indoor power-line channels," in *Proc. IEEE International Symposium on Power Line Communications and Its Applications ISPLC '07*, March 2007, pp. 396–400.

[39] T. Miyawaki and C. W. Barnes, "Multirate recursive digital filters-A general approach and block structures," *IEEE Trans. Acoust., Speech, Signal Processing*, vol. 31, pp. 1148–1154, 1983.

[40] J. S. Prater and C. M. Loeffler, "Analysis and design of periodically time-varying IIR filters, with applications to transmultiplexers," *IEEE Trans. Signal Processing*, vol. 40, pp. 2715–2725, 1992.

[41] R. G. Shenoy, D. Burnside, and T. W. Parks, "Linear periodic systems and multirate filter design," *IEEE Trans. Signal Processing*, vol. 42, pp. 2242–2251, 1994.

[42] R. G. Shenoy, "Multirate specifications via aliasccomponent matrices," *IEEE Trans. Circuits Syst. II*, vol. 45, pp. 314–320, Mar 1998.

[43] C. Loeffler and C. Burrus, "Optimal design of periodically time-varying and multirate digital filters," *IEEE Transactions on Acoustics, Speech and Signal Processing*, vol. 32, no. 5, pp. 991–997, Oct 1984.

[44] P. P. Vaidyanathan, *Multirate System and Filter Banks.* Prentice-Hall, 1993.

[45] A. Saadat Mehr and T. Chen, "Representations of linear periodically time-varying and multi-rate systems," *IEEE Trans. Signal Processing*, vol. 50, pp. 2221–2227, 2002.

[46] G. Wang, "Analysis of M-channel time-varying filter banks," *Digital Signal Processing*, vol. 18, pp. 127–147, 2008.

[47] M. Abo-Zahhad, "Current state and future directions of multirate filter banks and their applications," *Digital Signal Processing*, vol. 13, pp. 127–147, 2003.

[48] M. J. T. Smith and T. P. Barnwell, "A new filter bank theory for time-frequency representation," *IEEE Trans. Acoustics, Speech, Signal Process*, vol. 35, pp. 314–327, 1987.

[49] D. C. McLernon, "One-dimensional linear periodically time-varying structures: derivations, interrelationships and properties," *IEE Proceedings - Vision, Image and Signal Processing*, vol. 146, no. 5, pp. 245–252, Oct. 1999.

[50] ——, "Properties for state-transition matrix of LPTV two-dimensional filter," *Electronics Letters*, vol. 38, no. 25, pp. 1748–1750, 5 Dec. 2002.

[51] ——, "Relationship between an LPTV system and the equivalent LTI MIMO structure," *IEE Proceedings - Vision, Image and Signal Processing*, vol. 150, no. 3, pp. 133–141, June 2003.

[52] W. Chauvet, B. Lacaze, D. Roviras, and A. Duverdier, "Characterization of a set of invertible lptv filters using circulant matrices," in *Proc. IEEE International Conference on Acoustics, Speech, and Signal Processing (ICASSP '03)*, vol. 6, April 2003, pp. 45–48.

[53] D. Roviras, B. Lacaze, and N. Thomas, "Effects of dicrete LPTV on stationary signals," in *Proc. IEEE International Conference on Acoustics, Speech, and Signal Processing (ICASSP '02)*, vol. 2, 2002, pp. 1217–1220.

[54] W. Yin and A. Saadat Mehr, "Least square identification of alias componentsof an lptv system," *to appear at IET Signal Processing*.

[55] ——, "Identification of linear periodically time-varying systems using periodic sequences," in *IEEE Multi-conference on Systems and Control 2009*.

[56] Z. T. Staroszczyk, "Power system time variance-LPTV model implementation and identification problems," in *11th International Conference on Harmonics and Quality of Power*, 2004, pp. 658–665.

[57] G. B. Giannakis and A. V. Dnizdawate, "Polyspectral analysis of (almost) cyclostationary signals: LPTV system identification and related applications," *Proc. 25th Asilomar Conf. on Signals, Systems, and Computers*, vol. 1, pp. 377–382, 1991.

[58] Y. Dorfan, A. Feuer, and B. Porat, "Modeling and identification of LPTV systems by wavelets," *Signal Processing*, vol. 84, pp. 1285–1297, 2004.

[59] M. K. Tsatsanis and G. B. Giannakis, "Time-varying system identification and model validation using wavelets," *IEEE Trans. Signal Processing*, vol. 41, pp. 3512–3522, 1993.

[60] M. Verhaegen and X. Yu, "A class of subspace model identification algorithms to identify periodically and arbitrarily time-varying systems," *Automatica*, vol. 31, pp. 206–216, 1995.

[61] J. Wang and T. Chen, "Multirate sampled-data systems: compute fast-rate models," *Journal of Process Control*, vol. 14, pp. 79–88, 2004.

[62] A. D. Samsb and V. Z. Marmarelis, "Identification of linear periodically time-varying system-snext term using white-noise test inputs," *Automatica*, vol. 24, pp. 563–567, July 1988.

[63] M. I. Doroslovacki and H. Fan, "Wavelet-based linear system modeling and adaptive filtering," *IEEE Transactions on Signal Processing*, vol. 44, no. 5, pp. 1156–1167, May 1996.

[64] K. Liu, "Identification of linear time-varying systems," *Journal of Sound and Vibration*, vol. 206, pp. 487–505, October 1997.

[65] F. Felici, J.-W. vanWingerden, and M. Verhaegen, "Subspace identification of MIMO LPV systems using a periodic scheduling sequence," *Automatica*, vol. 43, pp. 1684–1697, 2007.

[66] J.-W. van Wingerden and M. Verhaegen, "Subspace identification of bilinear and LPV systems for open- and closed-loop data," *Automatica*, vol. 45, pp. 372–381, February 2009.

[67] S. Mirabbasi, B. Francis, and T. Chen, "Controlling distortions in maximally decimated filter banks," *IEEE Transactions on Circuits and Systems II: Analog and Digital Signal Processing*, vol. 44, no. 7, pp. 597–600, July 1997.

[68] B. Yu, Y. Shi, and H. Huang, "l_2-l_∞ filtering for multirate systems based on lifted models," *Circuits, Systems, and Signal Processing*, vol. 27, no. 5, pp. 699–711, October 2008.

[69] M. Kawamata, X. Yang, and T. Higuchi, "Fundamental study on periodically time-varying state-space digital filters-statistical analysis, scaling and stability," in *Proc. IEEE International Conference on Systems Engineering*, Sept. 1992, pp. 348–351.

[70] L. L. Scharf, *Statistical Signal Processing: Detection, Estimation, and Time Series Analysis*. Addison-Wesley Pub. Co., 1991.

[71] P. P. Vaidyanathan, "Multirate digital filters, filter banks, polyphase networks, and applications: A tutorial," in *Proceedings of IEEE*, vol. 78, 1990, pp. 56–78.

[72] P. P. Vaidyanathan and A. Kirac, "Cyclic LTI systems in digital signal processing," *IEEE Trans. Signal Processing*, vol. 45, pp. 433–447, 1999.

[73] G. Xu, H. Liu, L. Tong, and T. Kailath, "A least-square approach to blind channel identification," *IEEE Trans. Signal Processing*, vol. 43, pp. 2982–2992, 1995.

[74] A. H. Sayed, *Fundamentals of Adaptive Filtering.* John Wiley & Sons, Inc. and IEEE Press, 2003.

[75] S. Kay, *Statistical Signal Processing: Estimation Theory.* Prentice Hall, 1993.

[76] P. Stoica and O. Besson, "Training sequence design for frequency offset and frequency-selective channel estimation," *IEEE Trans. Signal Processing*, vol. 51, pp. 1910–1917, 2003.

[77] H. Minn and N. Al-Dhahir, "Optimal training signals for MIMO OFDM channel estimation," *IEEE Trans. Wireless Communications*, vol. 5, pp. 1158–1164, 2006.

[78] X. Ma, L. Yang, and G. B. Giannakis, "Optimal training for MIMO frequency-selective fading channels," *IEEE Trans. Wireless Communications*, vol. 4, pp. 453–466, 2005.

[79] X. Dai, "Optimal training design for linearly time-varying MIMO/OFDM channels modelled by a complex exponential basis expansion," *IET Communications*, vol. 1, pp. 945–953, 2007.

[80] M. Ghogho and A. Swami, "Training design for multipath channel and requency-offset estimation in MIMO systems," *IEEE Trans. Signal Processing*, vol. 54, pp. 3957–3965, 2006.

[81] A. Saadat Mehr and T. Chen, "Properties of linear switching time-varying discrete-time systems with applications," *Syst. Contr. Lett.*, vol. 39, pp. 229–235, 2000.

[82] Z. Q. Luo and W. Yu, "An introduction to convex optimization for communications and signal processing," *IEEE Journal Selected Areas In Communications*, vol. 24, pp. 1426–1437, 2006.

[83] C. Wolf, "Multivariate quadratic polynomials in public key cryptography," Ph.D. dissertation, Katholieke Universiteit Leuven, 2005.

[84] A. I. Barvinok, "Feasibility testing for systems of real quadratic equations," in *Proceedings of the twenty-fourth annual ACM symposium on theory of computing*, 1992, pp. 126–132.